This manuscript has been submitted for publication in *Earth Surface Processes and Landforms*. Please note that, despite having undergone peer-review, the manuscript has yet to be formally accepted for publication.

Effects of estuarine mudflat formation on tidal prism and large-scale morphology in experiments

Lisanne Braat *[1], Jasper R.F.W. Leuven[1], Ivar R. Lokhorst[1], and Maarten G. Kleinhans[1]

[1]Department of Physical Geography, Faculty of Geosciences, Utrecht University, Utrecht, The Netherlands

August 30, 2018

Abstract

Human interference in estuaries has led to increasing problems of mud, such as hyper-turbidity with adverse ecological effects and siltation of navigation channels and harbours. To deal with this mud sustainably, it is important to understand its long-term effects on the morphology and dynamics of estuaries. The aim of this study is to understand how mud affects the morphological evolution of estuaries. We focus on the effects of fluvial mud supply on the spatial distribution of mudflats and on how this influences estuary width, depth, surface area and dynamics over time. Three physical experiments with self-forming channels and shoals were conducted in a new flume type suitable for tidal experiments: the Metronome. In two of the experiments, we added nutshell grains as mud simulant, which is transported in suspension. Time-lapse images of every tidal cycle and DEMs for every 500 cycles were analysed for the three experiments. Mud settles in distinct locations forming mudflats on bars and sides of the estuary, where the bed elevation is higher. Two important effects of mud were observed: the first is the slight cohesiveness of mud that causes stability on bars limiting vertical erosion, although the bank erosion rate by migrating channels is unaffected. Secondly, mud fills inactive areas and deposits at higher elevations up to the high water level and therefore decreases the tidal prism. These combined effects cause a decrease in dynamics in the estuary and lead to near-equilibrium planforms that are smaller in volume and especially narrower upstream with increased bar heights and no channel deepening. This trend is in contrast with channel deepening in rivers by muddier floodplain formation. These results imply large consequences for long-term morphodynamics in estuaries that become muddier due to management practices, which deteriorate ecological quality of intertidal habitats but may create potential area for marshes.

*L.Braat@uu.nl

1 Introduction

Estuaries are tidally influenced coastal bodies of water that are connected to a river system supplying freshwater and sediments. Estuaries occur in a wide variety of planform shapes and shoal patterns, which are caused by inherited initial conditions and changing boundary conditions. However, it is still unclear how these conditions contribute to the evolution of estuaries and therefore a full understanding of their behaviour is still lacking. Understanding these natural dynamics is relevant for ecology, economy and flood safety, since intertidal areas are important ecological habitats and estuaries often have important shipping fairways to inland harbours that are located in densely populated areas. Many estuaries are heavily managed to balance these values, but there is a need to increase our understanding of the natural dynamics to improve management strategies.

Alluvial estuaries are typically flanked by mudflats and salt marshes (Dalrymple et al., 1992; Dalrymple and Choi, 2007). Mud has different erosional and depositional characteristics than sand and can, therefore, affect the morphology of estuaries. Recently, the interest in estuarine mud has increased, because many estuaries have been dealing with increased negative effects of mud (e.g. fluid mud, siltation of channels and harbours, higher turbidity reducing light penetration, the attraction of pollutants; Ridgway and Shimmield, 2002; Dijkstra et al., 2011; Van Maren et al., 2015, 2016). On the positive side, mudflats are very productive areas for flora and fauna, though vulnerable because of their low biodiversity (Costanza et al., 1993). Only very few studies consider the decadal to centennial effects of mud on the morphology of the estuary. Studying these long-term trends might give better insights in more sustainable or more efficient management strategies and the prediction of the long-term morphological behaviour may improve by accounting for mud. For example, if we can determine how tidal channels migrate over time in relation to the amount of cohesive mud in the system, we can perhaps better manage causes of hyper-turbidity and dredge more sustainably by migrating the shipping route in accordance with the natural trend of the estuary.

Previous research on the long-term morphodynamics of estuaries has mostly been conducted by numerical modelling (e.g. Lanzoni and Seminara, 2002; Hibma et al., 2003; Van der Wegen and Roelvink, 2008; Van der Wegen et al., 2008; Moore et al., 2009; Van der Wegen and Roelvink, 2012; Van der Wegen, 2013; Dam et al., 2016; Braat et al., 2017), whereas only few studies use physical experiments (Reynolds, 1887, 1889, 1891). Also, long-term field data are scarce and limited to decades rather than centuries. For such long timescales, only numerical modelling studies are available, but these may suffer from weaknesses such as neglected processes, numerical effects, imperfect transport predictors and the need for calibration of physics-based parameters (Baar et al., 2018). Additionally, these

studies rarely include mud because this has only become possible very recently (Le Hir et al., 2001; Van Kessel et al., 2011; Dam et al., 2013; Braat et al., 2017). Therefore, complementary to numerical models, additional approaches are necessary, such as physical models that form the entire landscape on scale within one flume.

Experiments with self-forming estuaries are rare, especially compared to the large number of delta experiments (e.g. Smith, 1909; Hoyal and Sheets, 2009; Grimaud et al., 2017), meandering river experiments (e.g. Friedkin, 1945; Tal and Paola, 2007; Braudrick et al., 2009; Van Dijk et al., 2013) and braided river experiments (e.g. Ashmore, 1991), and even compared to the few tidal channel and inlets experiments (Tambroni et al., 2005; Stefanon et al., 2010; Vlaswinkel and Cantelli, 2011; Kleinhans et al., 2015). Physical experiments with lightweight sediment have been conducted for filling of deltas and river floodplain (e.g. Peakall et al., 2007; Van Dijk et al., 2013; Hoyal and Sheets, 2009). Peakall et al. (2007) describes the necessity of cohesive fines in experiments to maintain a meandering planform. This was later explained by two effects: Braudrick et al. (2009) found that filling of floodplain by suspended sediment reduces the tendency to form chute cut-offs that are the onset of braiding. Van Dijk et al. (2013) found that adding cohesive sediment reduced erosion rates and increases bank strength, while overbank sedimentation and lateral accretion on point bars led to a reduction in chute cut-offs. The resulting reduction of width to depth ratio reduces the tendency to braid and leads to alternate bars associated with the onset of meandering. Hoyal and Sheets (2009) found that cohesive deltas show stronger channelisation, narrow channels, slower channel migration rates and therefore a more complex coastline. With these results in mind, we hypothesise that cohesive sediment deposits in estuaries will also reduce the tendency to form new channels, increase bank strength and limit the migration of channels similar to rivers and deltas.

The objective of this study is to identify the effects of cohesive sediment supply on the shape and development of estuaries. We specifically focus on the effect on large-scale parameters that determine landward tidal penetration, bar pattern and large-scale dynamics, such as width, depth and depth distribution, surface area, volume and cumulative erosion and deposition over time.

2 Methods

The results presented in this paper are derived from three experiments. The initial and boundary conditions of these experiments were based on the experience gained from 35 exploratory experiments with varying initial and boundary conditions. In the three experiments that are presented here, we changed the cohesive sediment supply to systemati-

cally explore the effects of this changing boundary condition. In this paper we will present an experiment with *only sand*, an experiment with a *low mud supply* and an experiment with a *high mud supply*. The experiment with only sand is also presented in Leuven et al. (2018a), where estuaries with growing forced tidal bars are shown to determine a non-ideal estuary planform, which serves as a reference experiment for this study.

2.1 Experimental setup and scaling

The experiments are conducted in the recently built flume, the Metronome, of 20 by 3 m in size, which drives tidal flow by periodic tilting of the entire flume (Fig. 1; Kleinhans et al., 2017b). Until now, it has always been difficult to study estuaries with physical models (Hughes, 1993; Kleinhans et al., 2012), due to scaling problems caused by tidal flow in addition to general scaling issues (Paola et al., 2009; Kleinhans et al., 2014a). Older tidal experiments without the periodic tilting mechanism had a tendency to exclusively form ebb dominated, sediment-exporting systems (as reviewed in Kleinhans et al., 2012). Furthermore, these experiments suffered from low sediment mobility and bar-forming tendencies were often overwhelmed by a significant number of scour holes and small bedforms, probably due to hydraulic smooth conditions (Kleinhans et al., 2017a). The recently developed Metronome flume prevents these scaling issues by obtaining appropriate hydraulic similarity and sediment mobility, and therefore sediment transport similarity, in agreement with proven scaling methods that are required to obtain morphologic similarity (Peakall et al., 1996; Paola et al., 2009; Kleinhans et al., 2014a). In particular, we solved a classic scaling conflict between sediment friction and sediment mobility by using a coarse sediment to prevent hydraulic smooth conditions and associated scour holes (Kleinhans et al., 2017a) and at the same time increasing the Shields mobility number to similar values as found in nature by driving the periodic flow by periodic flume tilting (Kleinhans et al., 2017b) as explained below in detail. Pilot set-ups of this system have already been used in studies on tidal basins and ebb- and flood dominant channels (Kleinhans et al., 2012, 2014b, 2015), and the Metronome has also already been proven to be a more effective method of producing dynamic estuaries compared to solely vertical water fluctuations (Kleinhans et al., 2017b; Leuven et al., 2018a). Previous morphodynamic experiments showed that tidal bars scale similarly as tidal bars in natural systems: the length to width ratio and their correlation with local estuary width is in accordance with natural systems (Leuven et al., 2018a). However, the formation of cohesive tidal flats flanking non-cohesive channels within one experiment is novel in the experiments presented here.

The most important scale issue is that of sediment mobility. In scale-experiments where the spatial dimensions of

the system are reduced, the sediment often has a similar grain size as in nature, while the water depth is much smaller leading to a lower velocity and therefore lower sediment mobility. If sediment is scaled down similarly to water depth the physiochemical sediment properties would change; sand would become strongly cohesive clay. Therefore, it is common practice in river experiments to increase the slope of the flume to counteract the unscaled grain size to create realistic sediment mobility and as a result realistic transport rates (Peakall et al., 1996; Kleinhans, 2010). The problem in tidal experiments is that water and sediment should be transported in two directions and therefore an increased slope would only favour ebb-related transport. By using the novel tilting method of the Metronome, this is avoided. During ebb flow, the flume is tilted seaward while during flood the flume is tilted landward. With this method we obtain peak Shields numbers of 0.15-0.2 for sand, which is well above the beginning of motion and close to that of small natural estuaries, obtaining sediment transport similarity while maintaining subcritical flow (Kleinhans et al., 2017b). In theory, decreasing the density of the sediment is also a possibility to reduce most of these scaling issues. However, using, for example, plastic sediment is unfavourable for experiments with mud or vegetation and leads to practical problems of cost and waste treatment. The tilting method is based on several pilot studies in smaller flumes (Kleinhans et al., 2012, 2014b, 2015) and a more extensive description, operation and technical information of the flume can be found in Kleinhans et al. (2017b).

2.2 Boundary and initial conditions

The tilting amplitude of the metronome is 75 mm resulting in a maximum slope of 0.0075 mm^{-1} (or 0.75%) and tilts with a period of 40 s for the experiments with only sand and the experiment with a high mud supply. The experiment with a low mud supply was subjected to a slightly lower tilting amplitude of 68 mm, but the same period. Tilting amplitude and period were chosen so that sediment mobility was ensured for correct scaling and the tidal excursion length was shorter than the length of the flume (see Kleinhans et al., 2017b, for description and comparison to natural systems). These values for tilting amplitude and period were chose on the basis of pilot tests with a range of tilting amplitudes and periods (see supplementary Fig. S1 and S2 for the results of these pilots). The mean water level was set 0.065 m above the flume floor and -0.005 m elevation relative to the land surface. The resulting water level amplitude of the experiments is 0.5-1 cm which is less than half the typical water depth of 3 cm, a similar ratio as natural systems (Savenije, 2015). Upstream we add a river discharge of 300 Lh^{-1} during ebb, and downstream we generate waves with a paddle during flood with a frequency of 2 Hz and 1 cm amplitude (supplement of Leuven et al., 2018a). The

river discharge alone is not strong enough to transport sand in the flume in absence of tilting (supplementary Fig. S3b). However, when tilting is applies without river discharge a closed, short tidal basin develops (supplementary Fig. S3c), showing that a minor river discharge is essential to develop an elongated estuary. The experiment starts with a bed thickness of 7 cm that consists of only sand with an exponential widening shape of 3 cm deep (bottom Fig. 1). The initial shape decreases from 1 m width at the mouth of the estuary to 0.2 m at the river end with a characteristic e-folding convergence length of 3 m. The bottom of the flume is covered with artificial grass. If scours develop that reach the bottom of the flume, the roughness of the grass prevents further erosion in this location. The basin area in which the ebb delta can expand during the experiment is 2 m long. Water levels in the flume are controlled by a weir at the end of the flume while pumps constantly add water to the sea basin. This weir compensates for the tilting of the flume by maintaining a horizontal water level (constant head) in the sea between the end of the flume and the front of the ebb delta at all times. Because the ebb delta grows the compensation of the weir is adjusted during the experiment. Water flowing out of the flume is recirculated. The total duration of each experiment is 15,000 tidal cycles.

The experiment with the low nutshell supply had a slightly lower tilting amplitude than the other two experiments. Instead of 75 mm, this experiment used a tilt of 68 mm. This was due to an accidental software update of the Metronome during the period the experiments were carried out, which was only discovered after the experiment was finished. Based on pilot studies focussed on amplitude variations, we do not expect that this error influences the main outcomes of this study. However, we expect that the resulting estuary might be slightly shorter and smaller. The effect of tilting amplitude on estuary length is indicated by pilot experiments shown in supplementary Fig. S1. The length of the estuaries is proximately constant throughout the experiments, in contrast to estuary width.

2.3 Sediment characteristics

To simulate mud in the experiment we used nutshell grains (as used in Baumgardner, 2016; Ganti et al., 2016; Van de Lageweg et al., 2016; Baar et al., 2018). Pre-wetted nutshell was added to the system during ebb with the river discharge. We conducted an experiment with a low concentration of 1 ml nutshell per cycle (0.405 g/L) and an experiment with a high concentration of 5 ml nutshell per cycle (2.025 g/L). In total 12 kg and 60 kg of nutshell was supplied to these experiments over 15,000 cycles. However, not all nutshell deposited in the estuaries, but also a large part was transported out of the estuary and settled in the ebb delta. Throughout the paper, we will refer to these experiments as the experiments with *low* and *high* mud supply concentration.

The nutshell was chosen to simulate mud because it is light-weight with a dry density of 1350 kgm^{-3} and therefore travels in suspension, and because it is only slightly cohesive. To test the exact cohesive effect of nutshell over time, we conducted bank erodibility tests with the method of Friedkin (1945) and the exact same setup as Van Dijk et al. (2013); Kleinhans et al. (2014a). Sediment samples created in the lab were subjected to a flow of 400 L/h under an angle of 45 degrees. Pictures were made every 10 seconds to track the volume of the sample over time and to measure the erosion rate. The samples that were tested were 10x37 cm with a triangular corner cut off of 10x10 cm. The samples were made of a combination of 4/5 sand and 1/5 nutshell on top and were kept under similar circumstances as in the Metronome for a variable number of days. To create similar circumstances the samples were almost fully submerged with recirculating water flow with approximately the same amount of anti-algae and chlorine that was used in the Metronome. As other authors suggest, the nutshell is indeed non-cohesive if subjected to experimental condition for only a short time (as mentioned by Ganti et al., 2016). However, mud deposits became more difficult to erode due to slight decomposition over time and perhaps fungal development, as in natural estuaries where the critical shear stress for erosion increases over time due to consolidation and biofilm development (Torfs et al., 1996).

Sand in the experiments has a median grain size of 0.55 mm with a D_{10} of 0.32 mm and a D_{90} of 1.2 mm (see for design Kleinhans et al., 2017b). The sand mixture was prepared by wet sieving which completely removed any fines below 0.125 mm. There was no sand supply upstream. The nutshell has a grain size of 0.2 mm. Preliminary test with the nutshell indicated that coarse nutshell (1.3–1.7 mm) not only settles with low velocities but also deposits when the grain size is larger than the water depth on bars. We hypothesise that this effect might be the cause for the different point bar deposits for nutshell and silt in Van de Lageweg et al. (2016), where nutshell deposited dominantly on the downstream half of the point bar, while the silt deposited in the upstream half. A much smaller nutshell grain size was used for the estuary experiments and solved this difference between the silt and nutshell behaviour. This means that we are simulating a finer fraction than in the river experiments by Van de Lageweg et al. (2016).

2.4 Data collection and analysis

Time-lapse images were collected using 7 AVG Mako (G-419C) colour cameras on the ceiling. All images have a resolution of 2048 by 2048 pixels with a footprint of about 3.15 m resulting in a pixel resolution of approximately 1.5 mm. The images were taken every tidal cycle when the bed was horizontal. Pre-processing of the images included: debayering of the original Bayer images, noise removal, lens correction (vignette and distortion), geometric

rectification, colour, contrast and brightness correction after which the images were stitched together. The water was dyed blue with food colouring to get an impression of water depth from the top view photographs. Additional images were obtained every 500 to 1000 tidal cycles when we temporarily drained the experiment. This way the nutshell was classified more easily, compared to the images with water. Mud was classified per pixel only based on colour thresholds in the images without water.

A digital Canon SLR camera was used to collect oblique photos of the experiment. These photos were used to make digital elevation models (DEMS) by structure from motion software Agisoft PhotoScan (version 1.2.6.2038) and were referenced with 20 ground control points along the sides of the flume at a 2 m interval. In the analysis of the DEMs unaffected areas of the flume were masked and the ebb delta was excluded unless stated differently.

Particle image velocimetry (PIV) on floating plastic particles was used to obtain surface water velocities in the entire flume at 16 phases (every 22.5 degrees) of the tidal cycle. Ten images were taken every phase with a sampling frequency of 25 Hz. The MPIV Matlab toolbox was used to calculate the velocities from the floating particles. PIV measurements were performed every 500 to 1000 cycles in the experiment without nutshell up to cycle 8863 and at the end of the experiment with a low input concentration of nutshell. There are no PIV measurements during the experiments with nutshell because the removal of the plastic particles influenced the mud deposits. During pre-processing of the PIV images, lens correction was done before the velocities were calculated from the displacement of the particles, but geometric rectification and stitching of the velocity data from different cameras were done afterwards due to memory issues. Additionally, the tilt of the Metronome was not taken into account, but since discontinuities are barely visible in the stitched images, we assume that the projection errors are negligible.

During post-processing, the peak velocity ratio was calculated from the ratio between the maximum ebb and flood velocities. To make the colour-scale more readable we took the negative reciprocal $(-1/x)$ of the values between 0 and -1 so that ebb dominant would be negative and flood dominant positive. If only flood or only ebb flow was measured, no ratio was calculated and therefore plots as zero. For example, highly elevated shoals sometimes flood and drain in the same direction, because maximum high water does not occur at exactly the same time as slack water.

3 Results

We will first describe the general evolution of the estuary in several phases. This is followed by an analysis of the location of mud deposits and the effects of the mud in the estuary.

3.1 General estuary evolution

The development of the experimental estuary exists of four phases. In the first phase of the experiments, the exponentially converging channel starts to develop a channel-shoal pattern. This pattern develops within approximately 100 tidal cycles resulting in an alternate bar pattern (Fig. 2a-c). At the same time, the ebb delta starts to form and continues to grow throughout the experiment. Sand is collected in the middle of the flume, caused by a lack of sediment input upstream and downstream and an estuary planform that does not exactly fit the imposed hydrodynamic conditions (Fig. 3). At the end of this phase, the estuary contains one big meandering channel with sills between bends (cycle 300, Fig. 2a-c).

In the second phase, the estuary widens rapidly by outward and downstream migration of tidal meanders (Fig. 4). In some places, there is little lateral widening over time and in some places, there is a large lateral extension of the tidal meanders. The width generally decreases in the upstream direction even though there local areas that are wider (Leuven et al., 2018a). In addition, the bed profile changes to a more linear profile by reworking of the initial bulge (Fig. 3). Although there is some downstream bend migration, this is limited to the initial phase of the experiment. The widening of the estuary favours the formation of multiple channels and bars across the estuary. Small flood channels that end on bars, named barb channels, increase in size and develop into connected ebb and flood dominated channels (Leuven et al., 2018a, cycle 800, Fig. 2d-f;). After about 1800 tidal cycles these multiple channels become clearly visible as a weakly braided pattern (Fig. 2g-i).

In the third phase from cycle 3300, the first effects of the mud are observed on the estuary width (Fig. 4, 2j-l). The first mudflats start forming in the upper part of the estuary and slowly spread further downstream. They, however, settle rarely in the lower estuary due to the large reworking of sediment in the area and constantly migrating channels and bars.

In the fourth phase and final state, the morphology after 15,000 tidal cycles for the three experiments is a self-formed, freely-erodible, bar-built estuary with migrating channels and bars (Fig. 2II-IV). The experiments approach dynamic equilibrium from cycle 10,900 (Fig. 2v-x), because we see a levelling of the cumulative sedimentation and erosion (Fig. 5). In the final state, the width of the estuary generally decreases in the upstream direction (Fig. 4) and the bed profile increases linearly (Fig. 3). The typical resulting channel depth at the mouth is 4 cm and average bed levels are 2 to 2.5 cm at the mouth of the estuary (Fig. 3). Typical velocity amplitudes are 0.3–0.4 ms^{-1} (Fig. 6 and 7), with maximum velocities occurring in the deepest channels downstream (Fig. 6). However, width-averaged velocity

amplitudes are lower downstream than upstream.

3.2 Mudflat characteristics

The experiments with mud supply resulted in estuaries with self-formed mudflats. The nutshell particles settle on the highest elevations of intertidal areas and form mudflats (or 'nutflats'). The mudflats occur on bars and flank the estuary (Fig. 8 and Fig. 9). The flats can be recognised by an orange to brown colour which is related to the time the mud has been in the system. We observe mud deposits on all types of bars, for example, mid-channel bars (Fig. 9a, b and e), scroll bars (Fig. 9c) and sidebars (Fig. 9d and e). On the bars, mud first settles at the highest locations after which the flat spreads to lower elevations if it can grow in size.

The mud supplied upstream is self-distributed throughout the whole estuary, but mostly settles in the upstream regions (Fig. 8). Initially, mud only deposits upstream, which results here in relatively high percentages of mudflats (Fig. 10). For the experiment with high mud supply, the fraction upstream of 10 m after only a few hundred cycles is already approximately 40%. Over time the mudflat area increases upstream and gradually extends more downstream as well, which is especially clear in Fig. 10b, where the front between low and high percentages of mud moves downstream over time. In this experiment, a large volume of mud settles in the lower estuary, but the coverage is still less than 50% of the estuary width (Fig. 10).

For the experiment with a higher mud supply, we observe that mudflats are, as expected, larger and more abundant, as high as 12.5 m^2, compared to 3 m^2 for the experiment with low mud supply (Fig. 8). Relatively this is a mud coverage of 62% of the surface area for the experiment with high mud supply and 15% for the experiment with low mud supply, which is consistent with the fact that the high mud supply is five times larger than the low mud supply. Additionally, the downstream spreading occurs faster (Fig. 10). After about 8000 cycles the upstream part is so dominated by mud that it also deposits in the channels (Fig. 8). This means that the relative mud cover approaches 100% (Fig. 10).

Initially, mud only deposits at high elevations between -1.5 and -0.5 cm near the observed high water level, mostly on bars (Fig. 11, dotted lines). Over time this lower knick point in Fig. 11 (dotted lines) becomes weaker and decreases to about -2.2 cm for the highest supply. We hypothesise this is due to different kind of deposits later in the experiments (e.g. filling of abandoned channels). However, the majority of the mud is still located between -1.5 and -0.5 cm.

3.3 Mud preservation

To understand which areas in the estuary are influenced most by mud, we investigated which mud deposits are most stable. The age of mud could be estimated by combining the mud maps to indicate the stability of the mudflats (Fig. 12). We assume that mud was not eroded and redeposited between two images. From this data we can see that some upstream bars show a pattern: first, a small flat develops and then this mudflat expands in the upstream direction and to lower elevations. In the middle of the estuary, the mudflats are very stable in location and size, and some locations have been stable since the beginning of the experiment (for about 15,000 cycles). Downstream, the mudflats are much younger in age (about 2000 cycles) due to larger dynamics of the channels. A small remnant of old mud remained at 9 m (Fig. 12a). This is a remnant of a larger mudflat that has disappeared due to the downstream migration of the biggest channel. Other analysis showed that mud deposits initially at a lower range of elevations as well but is only preserved at high elevations for a long time since older mud deposits occur at higher elevations, which is consistent with our explanation based on velocities and water levels. This is in contrast with rivers, where mud will never deposit at larger depths due to unidirectional flow, except in closed residual channels.

3.4 The effect of mud on morphodynamics

3.4.1 Bank erosion and erosion rates

The channel banks showed steep cliffs at the edges of bars that were subjected to erosion, which is evidence that the nutshell has some cohesive properties. We observed preferential erosion of sand over the nutshell at the bar margins (Fig. 9f). Sand was eroded from bar margins by undercutting of the mud layer on top of the flat after which the mud eroded by small collapses. This is in contrast with the gentler sloping sandy bar margins.

The Friedkin (1945) erosion tests were used to determine the exact effect of the mud on bank erosion. In this case, it behaves as non-cohesive, light-weight sediment as for example plastic sediments that transported and more easily than sand. However, when we added a thin mud layer on top of a sand sample, we observe that after several days the grains stick together and form a mat. This mat becomes stronger over time and changes the erosion mechanism of the samples. Instead of slumping sand, we now observe oversteepening and collapsing (as in Fig. 9f).

Despite this difference, there were no significant differences in the erosion rate of the samples with and without mud layer and between different sample times (Fig. 13). Cohesive blocks that end up at the toe of the bank by collapses are immediately removed due to excess basal capacity as observed in similar experiments with cohesive silt

(Kleinhans et al., 2014a) and in the field (Rinaldi and Darby, 2007). The transport capacity in the channel is so large that the type of erosion does not affect the erosion rate in this setup. Cohesive blocks are transported as a whole and destroyed rapidly. Even though we do not observe decreased bank erosion with nutshell, we observe that cohesive mats prevent erosion of mud particles with lower velocities under a more gradual slope in the estuary experiments. This suggests that the mild cohesion may reduce channel initiation and incision on bar tops in the experiments, but does not directly confine the estuary laterally.

3.4.2 Bar accretion by mud deposition

Bar accretion is caused by mud deposition on bars. In the experiment without mud supply, the bars are >5 mm below the initial dry estuary margin and are therefore submerged during high tide. In contrast, the bars in the experiment with mud are 3-10 mm higher due to the mud deposits on top of the bars (Fig. 2). The bar accretion can be as high as 5 mm. This is clearly visible in Fig. 11 where the cumulative surface area below 0 to -0.5 cm is constant for the experiment without mud but changes for the experiments with mud. Moreover, the increase in elevation of the bars is visible in Fig. 3, where the 90^{th} percentile of the elevation is higher for the experiments with mud. Visual observations also confirmed that the top of the mudflats on bars changed from intertidal to supratidal (supratidal bar visible in Fig. 9a and b). This is also contributed to the decrease in tidal prism and tidal range which we will discuss later.

Because mud only settles at very low velocities and shear stresses (Torfs et al., 1996), the places for deposition are different than for sand (dotted lines in Fig. 7). During ebb flow, mud is supplied to the system and spreads downstream by river discharge. Mud settling occurs mainly during slack tide due to near zero flow velocities (below the critical threshold of mud mobility; Fig. 7), which occurs near maximum high and maximum low water. At mean and low water levels the flow is concentrated in the channels and mud deposits cannot be preserved here due to high peak velocities (Fig. 6b). Fig. 7 also shows that peak velocities below the mud mobility threshold only occur at high elevations. Everything that deposits during low water slack is immediately washed away again during the next flood, while deposits during high water slack are more likely to preserve. During high water, bars are flooded and velocities slow down. Mud settles at these high elevations during slack tide because the water depth is shallow and cannot be re-suspended during mean and low water levels.

Peak velocity ratios indicate that mud deposits during high water can be related to flood in the lower and ebb in the

upper estuary (Fig. 6d). Upstream, the river has a larger influence and therefore ebb asymmetry is observed for peak velocity over a large area. Around the tidal bars in the lower estuary, peak velocity asymmetry is flood-dominated (Fig. 6d). Duration asymmetry was less pronounced and is therefore not shown. Longer flood durations were observed in small barb channels that terminate on their landward end, however, clear patterns were hard to identify. It is known that duration asymmetry is especially important for fine sediments, so we assume that most mud is deposited during high water slack following the flood, with exception of the most upstream areas. Peak velocity and duration ratios could not be determined in areas where the flow was unidirectional and for supratidal areas.

3.4.3 Mud confines the estuary shape

Deposition of mud on bars and on the sides confines the estuary shape and therefore decreases the width and surface area, especially upstream where there is more mud present (Fig. 4 and 10). The effect on widening downstream is limited because less mud is deposited in this part of the estuary. Not only the width of the estuary is confined by mud, but also the total reworked surface area (maximum values in Fig. 11). Even though the specific tidal meandering leads to a wider estuary mouth of 2.75 m for the experiment with the high mud supply compared to 2.1 m and 1.5 m of the other experiments (Fig. 2), the surface area of that experiment is smaller than the experiment with only sand (Fig. 11a and c). The total estuary area without mud increases up to 25 m^2, whereas the area of the experiments with mud cover an area of only 20 m^2 (Fig. 11). Surprisingly, the estuary with the high mud supply is roughly the same size as estuary with low mud supply. This is probably caused by the difference in the geometry of the mouth, which is barely affected by mud and narrower for the experiment with low mud supply. However, we cannot exclude the possibility that this is due to the software error that led to reduced tilting amplitude in the experiment with low mud supply. We expect that under the correct tilting the experiment would have been slightly larger than the experiment with the high mud supply, but still smaller than the experiment with only sand due to the confinement and filling mechanism.

3.4.4 Mud decreases estuary dynamics

Mud decreases the dynamics of channels and bars. Channels initially migrate and shift rapidly within the estuary (Fig. 14), but when mudflats develop the lateral widening of the estuary at the mudflat comes to a halt (Fig. 14e and f). In the cross section of the low mud supply, a mudflat developed on the bottom side and for the high mud supply on the top side of Fig. 14e and f. The migration in the experiment without mud is sometimes so fast that not enough DEMS

were made to follow the channel displacement in the time-stack (Fig. 14d). Observations with a higher temporal resolution from the overhead imagery for sand only show that channels remain active and rework bars in specific zones over the entire length of the experiment (Leuven et al., 2018a).

The width changes of the estuary in Fig. 4 also shows decreasing dynamics due to mud. For all experiments it holds that initially the estuary largely widens (wider spaced lines) and the widening rate decreases over time (closer spaced lines) as the estuary dimensions get closer to equilibrium conditions (Fig. 4). This decrease in change is more pronounced for the experiments with mud because the mud has confined the estuary, which is then also sooner close to equilibrium with reduced dynamics (Fig. 5).

The addition of mud significantly decreases erosion rates within the estuary. Without mud the estuary exported 0.25 m^3 of sediment in total and with mud only approximately 0.17 m^3 (Fig. 5). The export is essentially continuous and there are no clear signs of net import. All data so far suggest that the created system is an exclusively exporting system, however visual observations confirmed landward sand movement during flood. This transport was apparently not enough to counteract export. Variations in the general trend of the lines in Fig. 5 are due to inaccuracies of the DEMs. Similar to the analysis of the surface area, the experiments do not show any evidence of decreasing sediment export for higher mud concentration. Both experiments 2 and 3 have similar exported sediment volumes and surface areas (Fig. 5), even though the shape of the mouth is especially different. Due to the tilting amplitude error, the export in the experiment with low mud supply may have been slightly smaller than expected.

4 Discussion

In this section, we will first describe the two effects of mud that impact the morphological evolution of the system. Next, we will discuss the implications of our findings on the understanding of natural systems, followed by a discussion of the novelty and contribution of this research to the current state of physical experiments simulating estuaries and experiments with mud.

4.1 Cohesive effect of mud

Two effects of mud were identified to cause morphological differences between estuaries with and without mud. The first effect is the minor apparent cohesion that increases over time because nutshell grains stick together the longer they are in the experiment. The grains form a mat-like structure. These cohesive effects cause small cliffs to form

and lead to different bank erosion processes that include oversteepening and mass failures (Rinaldi and Darby, 2007) in contrast to more gentle slopes and gradual erosion for sand. However, auxiliary bank erosion tests did not show a significant effect on erosion rate (Fig. 13). Small effects on the erosion rate are visually observed under low velocities on more gentle slopes.

Apparent cohesion can also be created by vegetation (Tal and Paola, 2007). Roots and extracellular polymeric substances (EPS) can stabilise banks similar to cohesive sediment. However, it is still unclear whether vegetation and mud together provide significant cohesion in tidal systems or only reduce the flood storage as discussed below (de Haas et al., 2018). On the one hand, vegetation and mud might settle in the same locations and therefore an additional strengthening effect might be limited. On the other hand, vegetation also reduces flow velocities by creating friction, which might increase significant amounts of mud deposition and more vegetation settling. Further investigation and experimentation of mud in combination with vegetation is part of our future work.

4.2 Filling effect of mud

The second, perhaps more important effect of mud is to fill space and reduce the tidal prism and the possibility for bar splitting. The results showed that mud deposits further increase the elevation of areas that are already relatively high in elevation. For example, sandbars become higher when mud is supplied to the system (Fig. 3). This result agrees with earlier work by numerical modelling of mud in estuaries (Braat et al., 2017). Like the cohesive effects, this deposition contributes to confining the estuary but additionally limits the tidal prism (Fig. 15). The prism is reduced because less water can flow through a cross-section because part of the cross section is now filled with mud. This effect is clearly visible in the upstream part of the estuaries where most mud is deposited. In Fig. 15 the local tidal prism for the experiment with only sand continues to grow up to a local tidal prism of 0.07 m^3 passing the 10 m cross-section. For the experiment with low mud supply, we also observe a growth in tidal prism, but less strong. The prism at 10 m grows up to 0.053 m^3. For the high mud supply experiment, we even observe a reduction of the tidal prism over time in the upper part of the estuary. The final local tidal prism at 10 m is 0.043 m^3 and only 60% compared to the tidal prism for only sand. Wobbles in these lines can be correlated to individual bends that influence the width of the estuary.

A surprising insight from these experiments is therefore the different effect of mud sedimentation in rivers and estuaries. In contrast with rivers where floodplain sedimentation causes the channel to deepen to accommodate the

same river discharge through a cross-section (Tal and Paola, 2007), in estuaries the tidal prism adapts to the decrease in cross-sectional area. With a decrease in tidal prism, sediment transport also decreases.

In addition to the filling mechanism water level decrease also contributes to tidal prism decrease over time. Because we do not have measurements of water levels, we could only visually observe a decrease in tidal range with time. A fixed high and low water level was assumed along the flume and in time to calculate tidal prism and is, therefore, an overestimation. The prism-reduction effect we describe is therefore probably stronger than visualised in Fig. 15. Tidal prism was calculated along the flume which we define as local tidal prism: the volume between low and high water upstream of this point (Fig. 15). In addition to the decrease in tidal prism by the filling effect of mud, we assume the water level decreases by increased friction in the estuary due to the filling and the development of more complicated bars and channels. According to Dalrymple and Choi (2007), this means that the estuary becomes more hyposynchronous: the friction of the bottom increases and the convergence is less strong leading to a stronger decrease in tidal range towards the tidal limit. This is in accordance with the positive feedback identified by de Haas et al. (2018): the formation of shoals simulates the deposition of more mud leading to a growth of supratidal areas (reduction of intertidal area) further stimulating the growth of new intertidal areas, ultimately increasing friction and reducing tidal prism. This mechanism predicts that, with enough sand and mud available, all estuaries eventually fill up (de Haas et al., 2018).

4.3 Implications for understanding natural systems

The depositional patterns of mud match the classical patterns described by Dalrymple et al. (1992); Dalrymple and Choi (2007). Mudflats are flanking the estuary and are depositing on bars, while the seaward part is largely free of mud citepdalrymple2007. In addition, when the results are compared to data from real-world estuaries we notice that for many real-world estuaries the relative extent of mudflats is larger upstream, similar to our experiments: Western Scheldt (McLaren, 1993, 1994), Ems-Dollard (Van Heuvel, 1991), Dovey (Baas et al., 2008), Severn (Allen, 1987) and the Salmon River estuary (Dalrymple and Choi, 2007). This trend was also observed in numerical models (Braat et al., 2017; Lokhorst et al., 2018). Since the field data supports the experimental results, the experiment can help us understand how the mudflats in the system are formed. Bars in estuaries are mostly built by sand, only when they get more stable, mud starts settling on top of the bars. The preferential settling of mud upstream is not due to supply location, because the mud is transported through the whole estuary and also ends up in the ebb delta. Less

mud deposits downstream are due to the larger velocities and larger dynamics in the lower estuary. We expect that a marine supply would lead to a similar spatial distribution between the mouth and the upper tidal limit.

When bars increase in elevation because of mudflat accretion, they can change from intertidal to supratidal due to the filling effect and decrease in water level. This has important implications for marsh formation. These areas could potentially be a starting point where pioneer marsh species can find their window of opportunity (Cao et al., 2017; de Haas et al., 2018). This was recently also concluded in a numerical modelling study of estuaries with mud and vegetation (Lokhorst et al., 2018). An important question related to vegetation and mud settling is if the vegetation supports mud settling, or the other way around, or both. Showing that we can create mudflats in these experiments partly solved this chicken-or-egg problem. At least vegetation is not necessary for extensive mudflats and to increase the elevation of tidal bars. In the Western Scheldt, the elevations of bars have been increasing over the past years and are often considered an undesired consequence of dredging and dumping (Cleveringa, 2013; De Vet et al., 2017). However, this study shows that this trend can also partly be attributed to changes in mud supply either by natural or anthropogenic changes.

Besides the increase in bar height, the results showed that mud supply also influences the width, size and dynamics of the estuary morphology. Due to the filling mechanism and reduction in tidal prism, the estuary becomes more confined. The reduction in width and size was also observed in numerical models with mud (Braat et al., 2017). Similar to the experiments, the dynamics of channels and bars also decreased in models with mud compared to estuaries with only sand. Observing the same trends with both methods strengthen the certainty of these findings.

However, some differences are also observed between the models and the experiments. The models (Braat et al., 2017) show predominantly deposits on the sides, while in the experiments most deposits are on bars instead of on the sides. This probably relates to the balance between the initial and boundary conditions. In the model, there is initial import into the system, while in the experiments the estuary is mostly exporting, despite the filling mechanism discussed earlier. Because the experiments are widening over time, mud is rarely deposited on the sides. An alternative hypothesis is that varying discharge is necessary to form flats on the sides, as seen for floodplain formation in river experiments (Van Dijk et al., 2013). The initial horizontal bed is not flooded during high water for mud to deposit as overbank deposits. We expect that the confining effect of the estuary would be greater if this type of deposit would be formed. This could be achieved, by for example adding spring and neap tides. Other similarities with river experiments were found in strengthening of banks, decrease in meandering and a decrease in chutes (Van Dijk et al.,

2013). However, since the prism adapts to the cross sections, we do not observe deeper channels as for rivers where the discharge through the cross-section is forced.

The numerical models indicate that confinement of the estuary by mud can lead to a dynamic equilibrium (Braat et al., 2017), but we did not find such equilibrium in the experiments yet. Although, the equilibrium for experiments with mud is probably closer than for only sand (Fig. 5). We hypothesise that the experiments could also reach an equilibrium if filling continues and friction would further increase, decreasing the tidal prism and tidal amplitude. If this is true, this would have important implications for estuary management. Since altering the system by dredging might constantly bring the estuary out of equilibrium. If the equilibrium dimensions of an estuary are known, bringing the estuary closer towards these dimensions will likely decrease the dynamics and will make maintenance of the shipping channel easier, while bringing the estuary out of equilibrium will only increase dynamics and will make maintenance of the shipping fairways more difficult.

While high mud concentrations are often seen as negative because of fluid mud, decreasing light penetration and silting up of harbours; some mud is important for ecology. Muddy areas are often the most biologically active areas of the estuary and an important part of the ecosystem (Costanza et al., 1993). These ecosystems can be largely affected by changes in mud supply concentration. The results show that if mud were absent, intertidal flats are lower and might drown species that prefer high intertidal or supratidal regions. Many benthic species also prefer a muddy substrate (Bouma et al., 2005). Results also suggest that if mudflats are absent the estuary will expand faster which might affect surrounding areas if there are no dikes bordering the estuary.

4.4 Novelty of mud in tidal experiments

The results showed an improvement in the methodology of conducting tidal experiments. Continuous dynamics were obtained with dynamic ebb and flood dominated channels that are typical for tidal systems. These channels were already described by van Veen (1950) and are essential for natural estuarine behaviour. It has been somewhat difficult to maintain dynamics in experiments in the past (Kleinhans et al., 2012; Vlaswinkel and Cantelli, 2011), but these experiments show dynamic channels without any extra trigger or irregular forcing. This is because the Metronome was successful in achieving sediment mobility along the whole estuary in both flow directions.

Of additional interest is that the shape and patterns are self-formed. Until now, the shape of the estuary was often imposed especially for numerical models (Hibma et al., 2003; Van der Wegen and Roelvink, 2008), but also

for experiments (Tambroni et al., 2005). The final shape of the estuary is a self-formed exponential shape with some deviations (Fig. 4). It is widely accepted that an exponential shape is the natural equilibrium planform of most natural estuaries (Lanzoni and Seminara, 2002; Savenije, 2015). However, observations in natural systems show that the width of estuaries can be rather irregular than ideal exponential Leuven et al. (2018b). The locations where the estuary is wider than ideal are locations where bars occur in natural systems, which is consistent with observations in the experiments Leuven et al. (2018a). These bars are intertidal areas and because flow velocity on the bars is low, they are also the places where mud is likely to settle when available. Therefore, the outline of the estuaries is a relevant indicator for the locations of mudflats, which also translates into predictable depth distributions Leuven et al. (2018c).

Idealised experimental studies like this are useful to get an understanding of the main processes that are involved in the morphological evolution of estuaries. These processes are hard to isolate from field data, and data is generally sparse. However, detailed results should be interpreted with caution as details in the natural morphology might be hampered by scale effects, such as the occurrence of scour holes (Kleinhans et al., 2017a) or are influenced by processes that were neglected, such as additional tidal components, inherited hard substrates, and salinity. These effects cannot presently be accounted for in large-scale system experiments.

A side effect of solving the mobility scaling problem with the tilting flume is that the water level variations are now caused by the flow instead of flow caused by water level variations. This means that the water level is no longer a simple function of the tides but a complex result of local friction and the wave of water going through the system as the flume tilts, while the typical phase relations for estuaries between flow and water level are lost (Kleinhans et al., 2017b).

Using nutshell as a proxy for mud also imposes limitations. The cohesive properties could not exactly be simulated at scale, because the degradation of the mud was poorly constrained because it depends on the temperature of the room, water, possibly inundation duration and the total time it has been in the flume. As a consequence, we believe that the cohesiveness of recently deposited nutshell was too low while it was too high for nutshell that had been in the flume for over 10,000 cycles. Since these older deposits were rarely subjected to large velocities, the effect on the final results was minimal, although perhaps the bars in the centre of the estuary might have been over-stabilised.

On the other hand, numerical models often also apply similar simplifications, such as ignoring multiple tidal components, multiple grain sizes, salinity and three-dimensional velocity calculations, especially for large time scales.

Even though scaling issues are absent, there are uncertainties in the physical representation of processes in models. To quantify these uncertainties and assess their effects, more studies with analogue experiments are desirable. The contribution of the present experiments is to complement the approach of numerical modelling.

5 Conclusions

The aim of the present research was to examine the effects of mud on the shape and dynamics of estuaries. Experiments in a novel tilting tidal flume, the Metronome, show that mudflat formation confines the morphology of the estuary. The main effect of mud is that it deposits in areas that would not be filled with sand otherwise and therefore decreases the local tidal prism, which, in turn, reduces the migration of channels and the large-scale widening of the estuary. As a result, the estuary becomes more confined as the width remains smaller, especially upstream, and total surface area of the estuary remains smaller with mud compared to only sand. Cohesive effects are surprisingly minor compared to the important role of cohesive floodplains on river patterns.

The second major finding was that mud increases the elevation of the bars and can transform bar surfaces from intertidal to supratidal. Bars and channels migrate slower and the estuary exports less sediment when mud is added to the system. Mud has a non-uniform spatial distribution along the estuary: more mud deposits upstream and therefore more morphological effects of the mud are observed upstream than downstream. In more detail, we found that mud is mostly deposited at intertidal bed elevations but preservation over time increases for higher elevations.

6 Acknowledgements

This research was funded by the Domain of Applied and Engineering Sciences TTW (grant Vici 016.140.316/13710 to MK) of the Netherlands Organisation for Scientific Research (NWO) and is part of the PhD project of LB. We would like to thank the technical staff of Physical Geography for their support, especially Arjan van Eijk, Chris Roosendaal and Marcel van Maarseveen for the daily problem solving and creative inventions. Wout van Dijk, Marcio Boechat Albernaz and Anne Baar are acknowledged for interesting discussions and comments on the manuscript. We gratefully acknowledge two anonymous reviewers for their constructive comments.

Authors contributed in the following proportions to concept and design, experiments, analysis and conclusions and manuscript preparation: LB(55,65,70,80), JL(10,30,10,0), IL(0,5,5,0) and MK(35,0,15,20).

References

Allen, J. (1987). Reworking of muddy intertidal sediments in the severn estuary, southwestern u.k.–a preliminary survey. *Sedimentary geology*, 50(1-3):1–23, doi:10.1016/0037-0738(87)90026-1.

Ashmore, P. E. (1991). How do gravel-bed rivers braid? *Canadian journal of earth sciences*, 28(3):326–341, doi:10.1139/e91-030.

Baar, A., de Smit, J., Uijttewaal, W., and Kleinhans, M. (2018). Sediment transport of fine sand to fine gravel on transverse bed slopes in rotating annular flume experiments. *Water Resources Research*, 54(1):19–45, doi:10.1002/2017WR020604.

Baas, J., Jago, C., Macklin, M., and CCCR Team (2008). The river-estuarine transition zone (retz) of the afon dyfi (west wales) as test bed for sediment transfer between river catchments and coastal environments. *BSRG 2008, December 14th-17th, Liverpool*.

Baumgardner, S. E. (2016). *Quantifying Galloway: Fluvial, Tidal and Wave Influence on Experimental and Field Deltas*. PhD thesis, University of Minnesota.

Bouma, H., De Jong, D., Twisk, F., and Wolfstein, K. (2005). Zoute wateren ecotopenstelsel (zes.1). Rapport RWS/RIKZ/2005.024, Ministerie van Verkeer en Waterstaat, Rijkswaterstaat, Middelburg.

Braat, L., Van Kessel, T., Leuven, J. R., and Kleinhans, M. G. (2017). Effects of mud supply on large-scale estuary morphology and development over centuries to millennia. *Earth Surface Dynamics*, 5(4):617–652, doi:10.5194/esurf-5-617-2017.

Braudrick, C. A., Dietrich, W. E., Leverich, G. T., and Sklar, L. S. (2009). Experimental evidence for the conditions necessary to sustain meandering in coarse-bedded rivers. *Proceedings of the National Academy of Sciences*, 106(40):16936–16941, doi:10.1073/pnas.0909417106.

Cao, H., Zhu, Z., Balke, T., Zhang, L., and Bouma, T. J. (2017). Effects of sediment disturbance regimes on spartina seedling establishment: Implications for salt marsh creation and restoration. *Limnology and Oceanography*, 63(2):647–659, doi:10.1002/lno.10657.

561 Cleveringa, J. (2013). Ontwikkeling mesoschaal westerschelde (factsheets). Basisrapport kleinschalige ontwikkeling
562 K-16 I/RA/11387/13.083/GVH, VNSC, International Marine and Dredging Consultants/Deltares/Svaek Hydraulics
563 BV/ARCADIS Nederland BV.

564 Costanza, R., Kemp, W. M., and Boynton, W. R. (1993). Predictability, scale, and biodiversity in coastal and estuarine
565 ecosystems: implications for management. *Ambio*, 22(2-3):88–96.

566 Dalrymple, R. W. and Choi, K. (2007). Morphologic and facies trends through the fluvial-marine transition in tide-
567 dominated depositional systems: a schematic framework for environmental and sequence-stratigraphic interpreta-
568 tion. *Earth-Science Reviews*, 81(3):135–174, doi:10.1016/j.earscirev.2006.10.002.

569 Dalrymple, R. W., Zaitlin, B. A., and Boyd, R. (1992). Estuarine facies models: conceptual basis and stratigraphic
570 implications: perspective. *Journal of Sedimentary Research*, 62(6):1130–1146, doi:10.1306/D4267A69-2B26-
571 11D7-8648000102C1865D.

572 Dam, G., Van der Wegen, M., Labeur, R., and Roelvink, D. (2016). Modeling centuries of estuarine morphodynamics
573 in the western scheldt estuary. *Geophysical Research Letters*, 43(8):3839–3847, doi:10.1002/2015GL066725.

574 Dam, G., Van der Wegen, M., and Roelvink, D. (2013). Long-term performance of process-based models in estuaries.
575 In *Proceedings Coastal Dynamics Conference 2013*, pages 409–420.

576 de Haas, T., Pierik, H., Van der Spek, A., Cohen, K., and Van Maanen, B. (2018). Holocene evolution of tidal systems
577 in the netherlands: Effects of rivers, coastal boundary conditions, eco-engineering species, inherited relief and
578 human interference. *Earth-Science Reviews*, 177:139–163, doi:10.1016/j.earscirev.2017.10.006.

579 De Vet, P., Van Prooijen, B., and Wang, Z. (2017). The differences in morphological development between the inter-
580 tidal flats of the eastern and western scheldt. *Geomorphology*, 281:31–42, doi:10.1016/j.geomorph.2016.12.031.

581 Dijkstra, J., van Kessel, T., van Maren, B., Spiteri, C., and Stolte, W. (2011). Setup of an effect-chain model for the
582 eems-dollard. Technical Report 1202298-000-ZKS-0002, Deltares.

583 Friedkin, J. (1945). A laboratory study of the meandering of alluvial rivers. Technical report, War Department, U.S.
584 Army Corps of Engineers.

585 Ganti, V., Chadwick, A. J., Hassenruck-Gudipati, H. J., Fuller, B. M., and Lamb, M. P. (2016). Experimen-
586 tal river delta size set by multiple floods and backwater hydrodynamics. *Science advances*, 2(5):e1501768,
587 doi:10.1126/sciadv.1501768.

588 Grimaud, J.-L., Paola, C., and Ellis, C. (2017). Competition between uplift and transverse sedimentation in an expe-
589 rimental delta. *Journal of Geophysical Research: Earth Surface*, 122(7):1339–1354, doi:10.1002/2017JF004239.

590 Hibma, A., De Vriend, H., and Stive, M. (2003). Numerical modelling of shoal pattern formation in well-mixed
591 elongated estuaries. *Estuarine, Coastal and Shelf Science*, 57(5):981–991, doi:10.1016/S0272-7714(03)00004-0.

592 Hoyal, D. and Sheets, B. (2009). Morphodynamic evolution of experimental cohesive deltas. *Journal of Geophysical*
593 *Research: Earth Surface*, 114(F2), doi:10.1029/2007JF000882.

594 Hughes, S. A. (1993). *Physical models and laboratory techniques in coastal engineering*, volume 7. World Scientific.

595 Kleinhans, M., Van der Vegt, M., Terwisscha Van Scheltinga, R., Baar, A., and Markies, H. (2012). Turning the tide:
596 experimental creation of tidal channel networks and ebb deltas. *Netherlands Journal of Geosciences*, 91(3):311–
597 323, doi:10.1017/S0016774600000469.

598 Kleinhans, M., Van Dijk, W., Van de Lageweg, W., Hoyal, D., Markies, H., Van Maarseveen, M., Roosendaal, C.,
599 Van Weesep, W., Van Breemen, D., Hoendervoogt, R., and Cheshier, N. (2014a). Quantifiable effectiveness of
600 experimental scaling of river- and delta morphodynamics and stratigraphy. *Earth-Science Reviews*, 133:43–61,
601 doi:10.1016/j.earscirev.2014.03.001.

602 Kleinhans, M., Van Rosmalen, T., Roosendaal, C., and Van der Vegt, M. (2014b). Turning the tide: mutually eva-
603 sive ebb-and flood-dominant channels and bars in an experimental estuary. *Advances in Geosciences*, 39:21–26,
604 doi:10.5194/adgeo-39-21-2014.

605 Kleinhans, M. G. (2010). Sorting out river channel patterns. *Progress in Physical Geography*, 34(3):287–326,
606 doi:10.1029/2005WR004674.

607 Kleinhans, M. G., Leuven, J. R., Braat, L., and Baar, A. W. (2017a). Scour holes and ripples occur below the hydraulic
608 smooth to rough transition of movable beds. *Sedimentology*, 64(5):1381–1401, doi:10.1111/sed.12358.

609 Kleinhans, M. G., Terwisscha van Scheltinga, R., Van der Vegt, M., and Markies, H. (2015). Turning the tide:
610 Growth and dynamics of a tidal basin and inlet in experiments. *Journal of Geophysical Research: Earth Surface*,
611 120(1):95–119, doi:10.1002/2014JF003127.

612 Kleinhans, M. G., Van der Vegt, M., Leuven, J., Braat, L., Markies, H., Simmelink, A., Roosendaal, C., Eijk, A.,
613 Vrijbergen, P., and Van Maarseveen, M. (2017b). Turning the tide: comparison of tidal flow by periodic sealevel
614 fluctuation and by periodic bed tilting in scaled landscape experiments of estuaries. *Earth Surface Dynamics*,
615 5(4):731–756, doi:10.5194/esurf-2017-11.

616 Lanzoni, S. and Seminara, G. (2002). Long-term evolution and morphodynamic equilibrium of tidal channels. *Journal
617 of Geophysical Research: Oceans*, 107(C1), doi:10.1029/2000JC000468.

618 Le Hir, P., Ficht, A., Jacinto, R. S., Lesueur, P., Dupont, J.-P., Lafite, R., Brenon, I., Thouvenin, B., and Cugier, P.
619 (2001). Fine sediment transport and accumulations at the mouth of the seine estuary (france). *Estuaries*, 24(6):950–
620 963, doi:10.2307/1353009.

621 Leuven, J., Braat, L., WM, V., De Haas, T., van Onselen, E., Ruessink, B., and Kleinhans, M. (2018a). Growing
622 forced bars determine non-ideal estuary planform. in review.

623 Leuven, J., Haas, T., Braat, L., and Kleinhans, M. (2018b). Topographic forcing of tidal sand bar patterns for irregular
624 estuary planforms. *Earth Surface Processes and Landforms*, 43(1):172–186, doi:10.1002/esp.4166.

625 Leuven, J., Selakovic, S., and Kleinhans, M. (2018c). Morphology of bar-built estuaries: relation between planform
626 shape and depth distribution. in review.

627 Lokhorst, I., Braat, L., Leuven, J., Baar, A., Van Oorschot, M., Selakovic, S., and Kleinhans, M. (2018). Morpholo-
628 gical effects of vegetation on the fluvial-tidal transition in holocene estuaries. in review.

629 McLaren, P. (1993). Patterns of sediment transport in the western part of the westerschelde. Technical report, GeoSea
630 Consulting, Cambridge, United Kingdom.

631 McLaren, P. (1994). Sediment transport in the westerschelde between baarland and rupelmonde. Technical report,
632 GeoSea Consulting, Cambridge, United Kingdom.

633 Moore, R. D., Wolf, J., Souza, A. J., and Flint, S. S. (2009). Morphological evolution of the dee estuary, eastern irish
634 sea, uk: a tidal asymmetry approach. *Geomorphology*, 103(4):588–596, doi:10.1016/j.geomorph.2008.08.003.

635 Paola, C., Straub, K., Mohrig, D., and Reinhardt, L. (2009). The unreasonable effectiveness of stratigraphic and
636 geomorphic experiments. *Earth-Science Reviews*, 97(1):1–43, doi:10.1016/j.earscirev.2009.05.003.

637 Peakall, J., Ashworth, P., and Best, J. (1996). Physical modelling in fluvial geomorphology: principles, applications
638 and unresolved issues. *The scientific nature of geomorphology*, pages 221–253.

639 Peakall, J., Ashworth, P. J., and Best, J. L. (2007). Meander-bend evolution, alluvial architecture, and the
640 role of cohesion in sinuous river channels: a flume study. *Journal of Sedimentary Research*, 77(3):197–212,
641 doi:10.2110/jsr.2007.017.

642 Reynolds, O. (1887). On certain laws relating to the regime of rivers and estuaries and on the possibility of experiments
643 on a small scale. Report, British Association.

644 Reynolds, O. (1889). Report of the committee appointed to investigate the action of waves and currents on the beds
645 and foreshores of estuaries by means of working models. Report, British Association.

646 Reynolds, O. (1891). Third report of the committee appointed to investigate the action of waves and currents on the
647 beds and foreshores of estuaries by means of working models. Report, British Association.

648 Ridgway, J. and Shimmield, G. (2002). Estuaries as repositories of historical contamination and their impact on shelf
649 seas. *Estuarine, Coastal and Shelf Science*, 55(6):903–928, doi:10.1006/ecss.2002.1035.

650 Rinaldi, M. and Darby, S. E. (2007). Modelling river-bank-erosion processes and mass failure mechanisms: progress
651 towards fully coupled simulations. *Developments in Earth Surface Processes*, 11:213–239, doi:10.1016/S0928-
652 2025(07)11126-3.

653 Savenije, H. H. (2015). Prediction in ungauged estuaries: An integrated theory. *Water Resources Research*,
654 51(4):2464–2476, doi:10.1002/2015WR016936.

655 Smith, A. L. (1909). Delta experiments. *Bulletin of the American Geographical Society*, 41(12):729–742,
656 doi:10.2307/199425.

657 Stefanon, L., Carniello, L., DAlpaos, A., and Lanzoni, S. (2010). Experimental analysis of tidal network growth and
658 development. *Continental Shelf Research*, 30(8):950–962, doi:10.1016/j.csr.2009.08.018.

659 Tal, M. and Paola, C. (2007). Dynamic single-thread channels maintained by the interaction of flow and vegetation.
660 *Geology*, 35(4):347–350, doi:10.1130/G23260A.1.

661 Tambroni, N., Bolla Pittaluga, M., and Seminara, G. (2005). Laboratory observations of the morphodyna-
662 mic evolution of tidal channels and tidal inlets. *Journal of Geophysical Research: Earth Surface*, 110(F4),
663 doi:10.1029/2004JF000243.

664 Torfs, H., Mitchener, H., Huysentruyt, H., and Toorman, E. (1996). Settling and consolidation of mud/sand mixtures.
665 *Coastal Engineering*, 29:27–45, doi:10.1016/S0378-3839(96)00013-0.

666 Van de Lageweg, W. I., Van Dijk, W. M., Box, D., and Kleinhans, M. G. (2016). Archimetrics: a quantitative
667 tool to predict three-dimensional meander belt sandbody heterogeneity. *The Depositional Record*, 2(1):22–46,
668 doi:10.1002/dep2.12.

669 Van der Wegen, M. (2013). Numerical modeling of the impact of sea level rise on tidal basin morphodynamics.
670 *Journal of Geophysical Research: Earth Surface*, 118(2):447–460, doi:10.1002/jgrf.20034.

671 Van der Wegen, M. and Roelvink, J. (2008). Long-term morphodynamic evolution of a tidal embay-
672 ment using a two-dimensional, process-based model. *Journal of Geophysical Research: Oceans*, 113(C3),
673 doi:10.1029/2006JC003983.

674 Van der Wegen, M. and Roelvink, J. (2012). Reproduction of estuarine bathymetry by means of
675 a process-based model: Western scheldt case study, the netherlands. *Geomorphology*, 179:152–167,
676 doi:10.1016/j.geomorph.2012.08.007.

677 Van der Wegen, M., Wang, Z. B., Savenije, H., and Roelvink, J. (2008). Long-term morphodynamic evolution and
678 energy dissipation in a coastal plain, tidal embayment. *Journal of Geophysical Research: Earth Surface*, 113(F3),
679 doi:10.1029/2007JF000898.

680 Van Dijk, W. M., Van de Lageweg, W. I., and Kleinhans, M. G. (2013). Formation of a cohesive floodplain
681 in a dynamic experimental meandering river. *Earth Surface Processes and Landforms*, 38(13):1550–1565,
682 doi:10.1002/esp.3400.

683 Van Heuvel, T. (1991). Sedimenttransport in het eems-dollard estuarium, volgens de method mclaren. Nota GWWS-
684 91.002, Rijkswaterstaat, dienst Getijdewateren.

685 Van Kessel, T., Vanlede, J., and De Kok, J. (2011). Development of a mud transport model for the scheldt estuary.
686 *Continental Shelf Research*, 31(10):S165–S181, doi:10.1016/j.csr.2010.12.006.

687 Van Maren, D., Oost, A., Wang, Z., and Vos, P. (2016). The effect of land reclamations and sediment
688 extraction on the suspended sediment concentration in the ems estuary. *Marine Geology*, 376:147–157,
689 doi:10.1016/j.margeo.2016.03.007.

690 Van Maren, D., Van Kessel, T., Cronin, K., and Sittoni, L. (2015). The impact of channel deepening and dredging on
691 estuarine sediment concentration. *Continental Shelf Research*, 95:1–14, doi:10.1016/j.csr.2014.12.010.

692 van Veen, J. (1950). Ebb and flood channel systems in the netherlands tidal waters. *Journal of the Royal Dutch*
693 *Geographical Society*, 67:303–325, doi:10.2112/04-0394.1.

694 Vlaswinkel, B. M. and Cantelli, A. (2011). Geometric characteristics and evolution of a tidal channel network in
695 experimental setting. *Earth Surface Processes and Landforms*, 36(6):739–752, doi:10.1002/esp.2099.

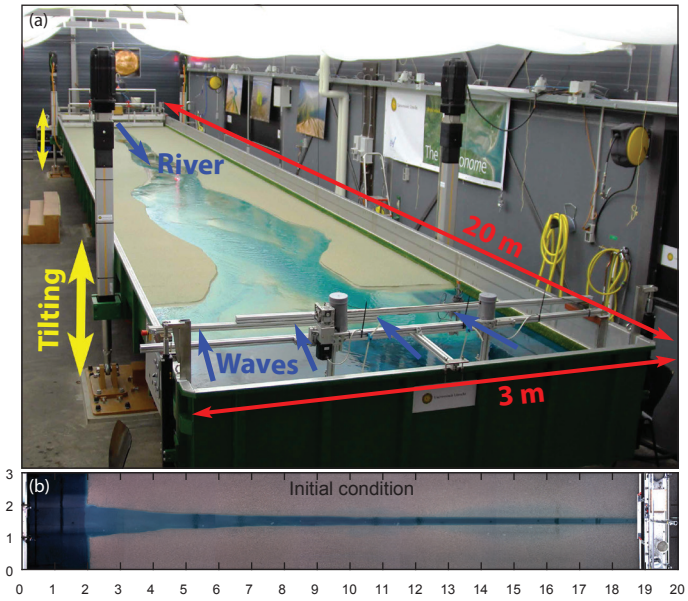

Figure 1: The Metronome: (a) the flume drives the flow by periodic tilting of the entire 20 by 3 m flume. Upstream input is river discharge and mud and downstream waves are generated. (b) Overhead imagery of the initial conditions with estuary mouth on the left and river on the right.

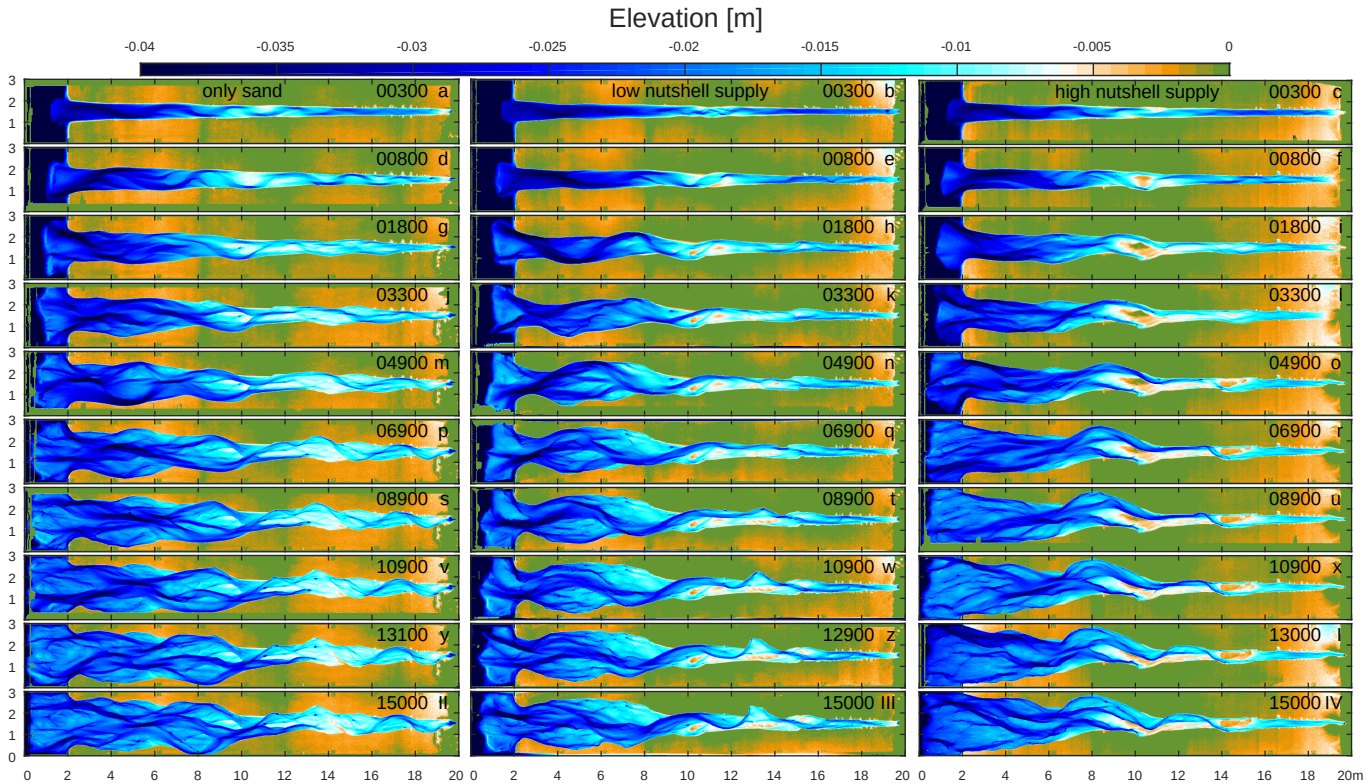

Figure 2: Time series of digital elevation models of the experiments without mud (left column), with a low mud supply (middle column) and a high mud supply (right column).

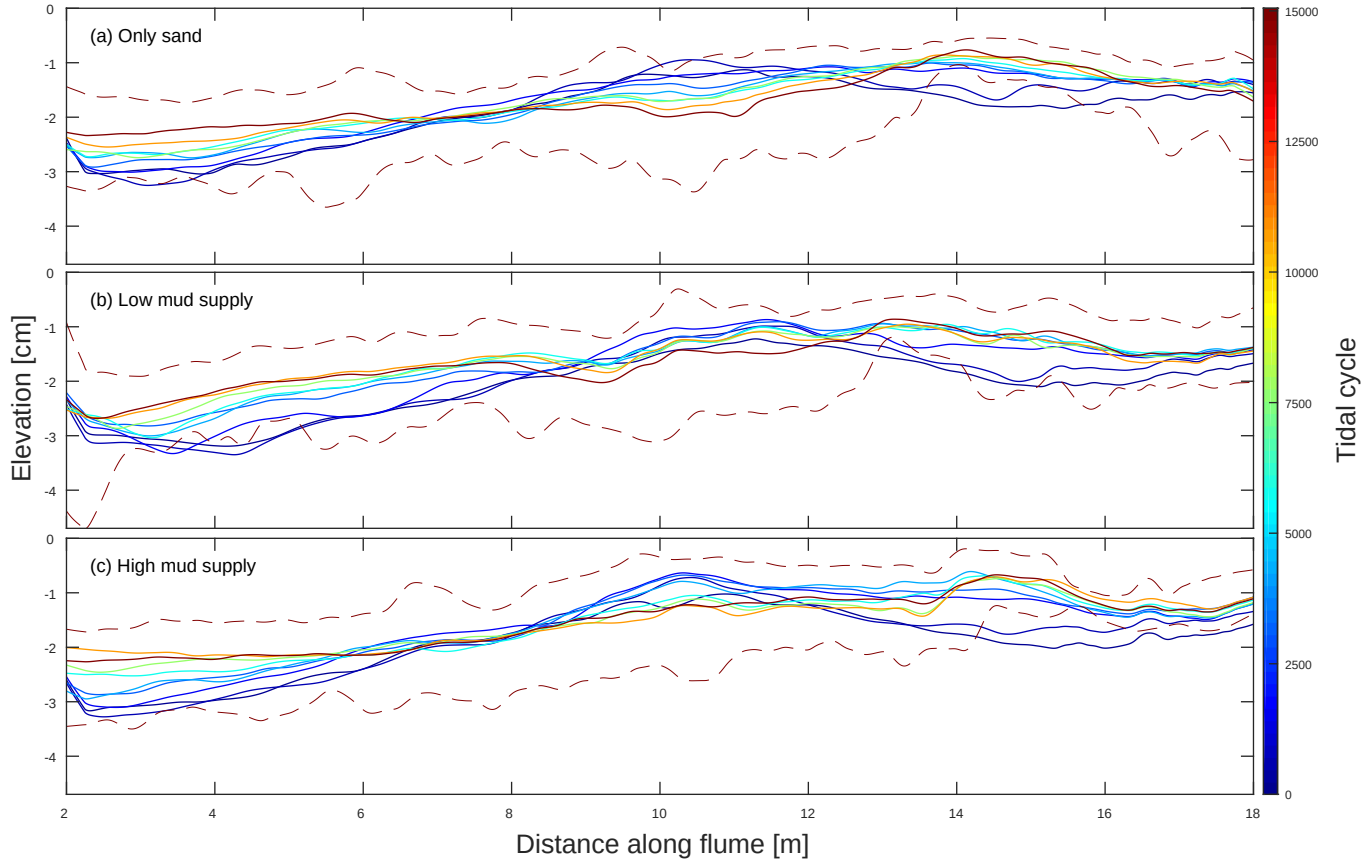

Figure 3: Mean (solid), 5 and 95 percentile (dashed) elevation along the estuary for the experiment with (a) only sand, (b) a low mud supply, and (c) a high mud supply indicating the evolution over time. Colours indicate different moments in time. The along bed elevation was median filtered over a length of 500 pixels, which equals 0.5 m.

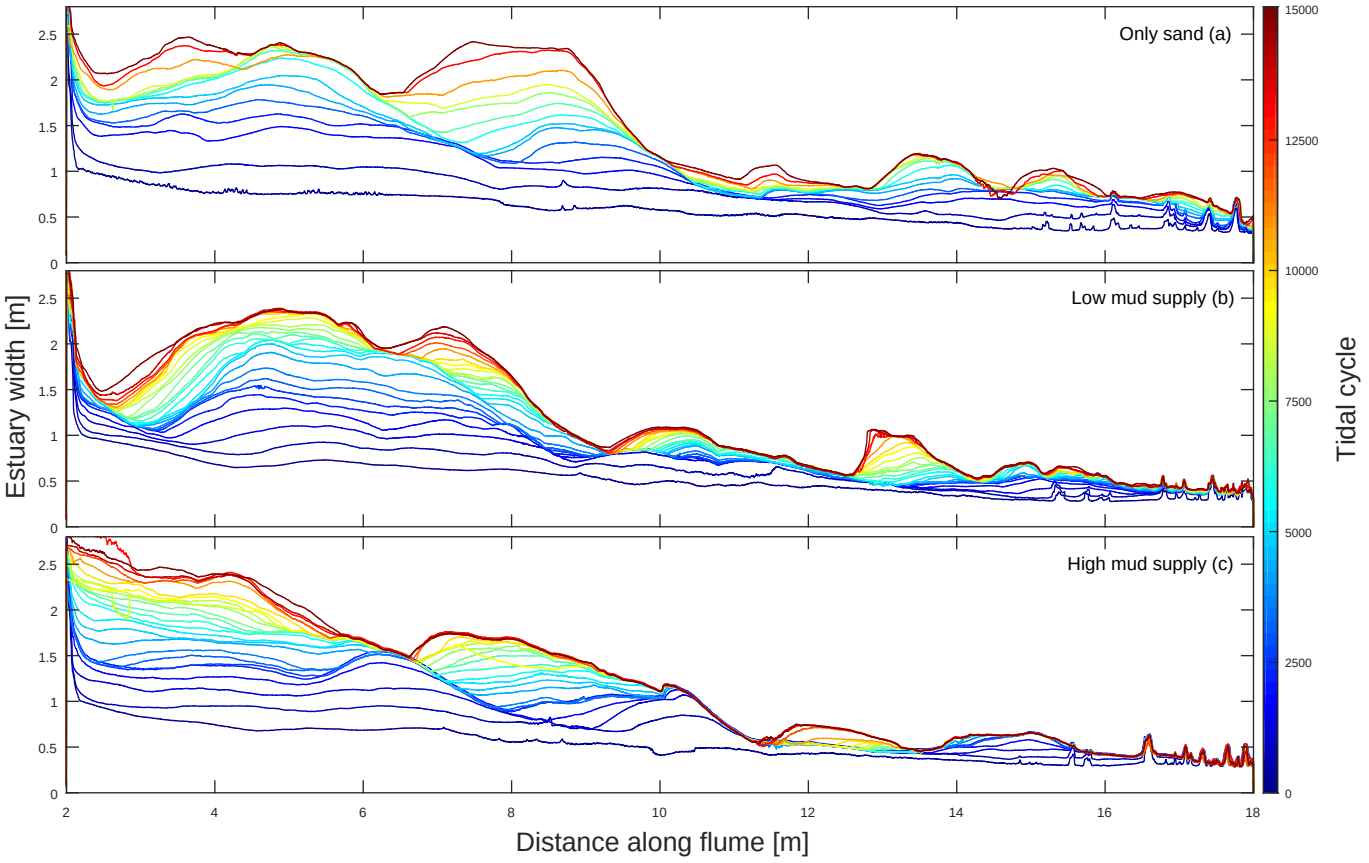

Figure 4: Width along the estuary for: (a) the experiment with only sand, (b) the experiment with a low mud supply, and (c) the experiment with a high mud supply. Colours indicate different moments in time.

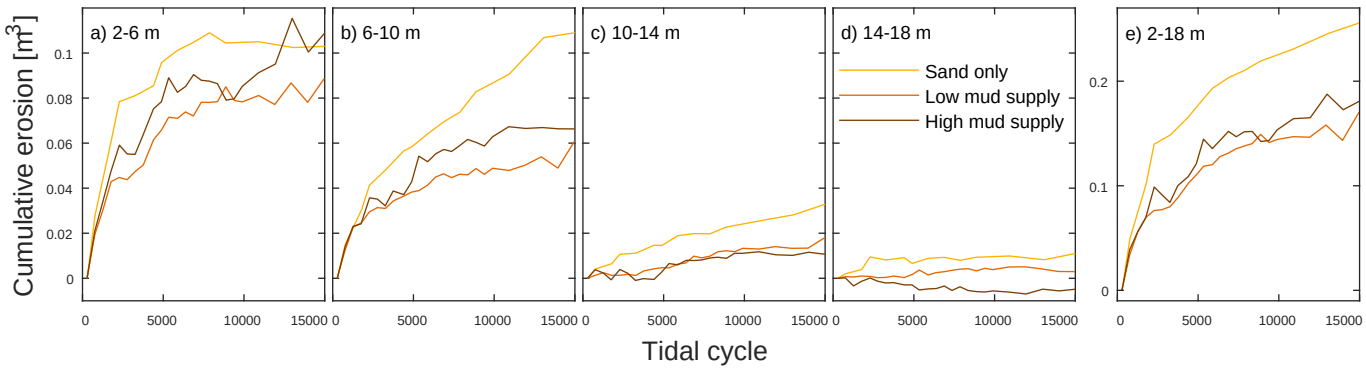

Figure 5: Cumulative sediment removed from the estuary over time for the three experiments, between (a) 2-6 m, (b) 6-10 m, (c) 10-14 m, (d) 14-18 m and (e) 2-18 m. Larger export occurred for the experiment with only sand. Experiments approach dynamic equilibrium.

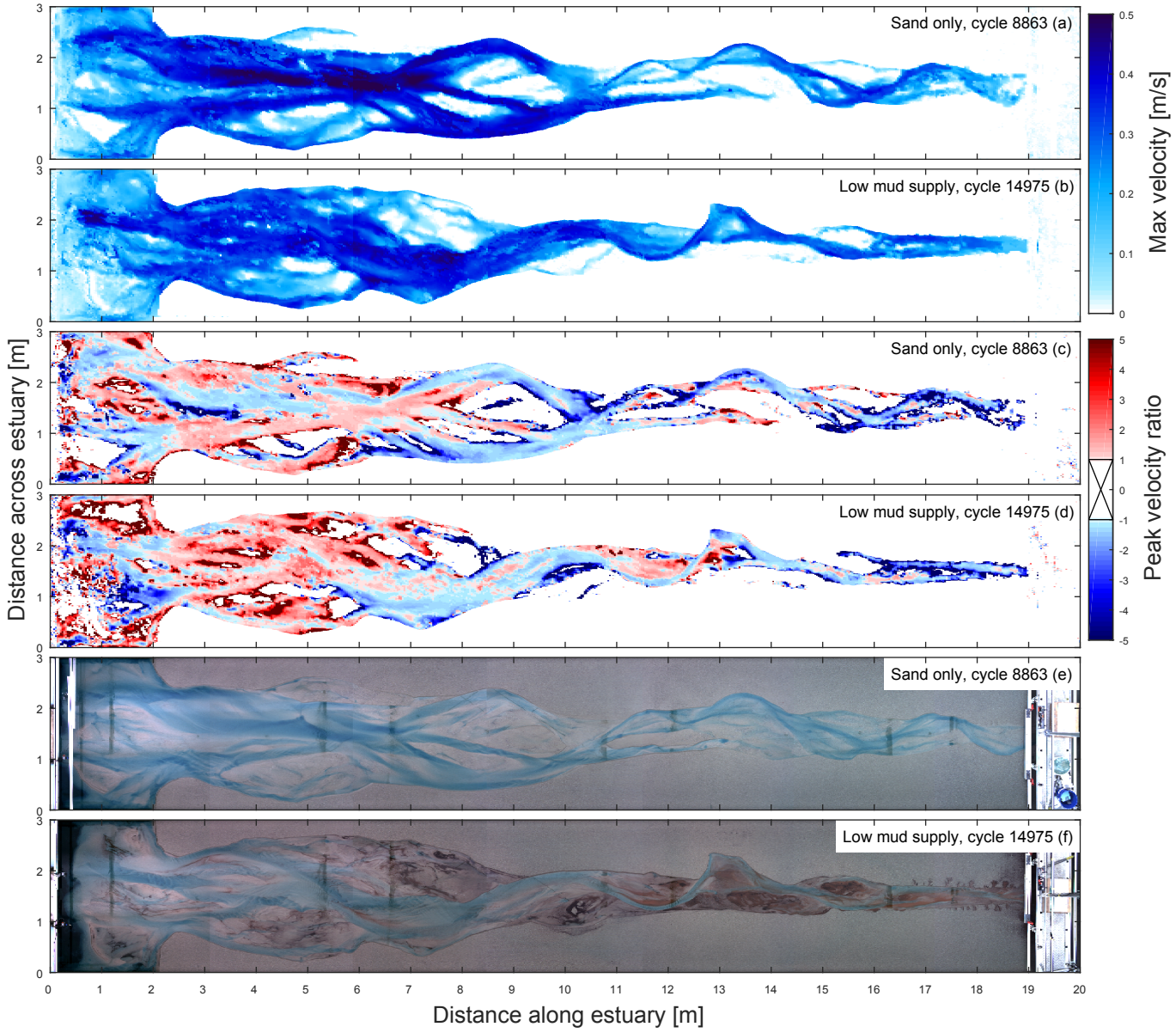

Figure 6: Maximum surface velocity over a tidal cycle for (a) sand only at cycle 8863 and (b) low mud supply at cycle 14975. Peak velocity ratio for (c) sand only at cycle 8863 and (d) low mud supply (b) at cycle 14975. Positive numbers indicate flood dominated and negative is ebb dominated. The number indicates the times the peak flood or ebb flow is larger than the flow in the other direction. No data if the flow was unidirectional or if the area was not flooded during the measurement. Related time-lapse images are shown in (e) for sand and (f) for low mud supply.

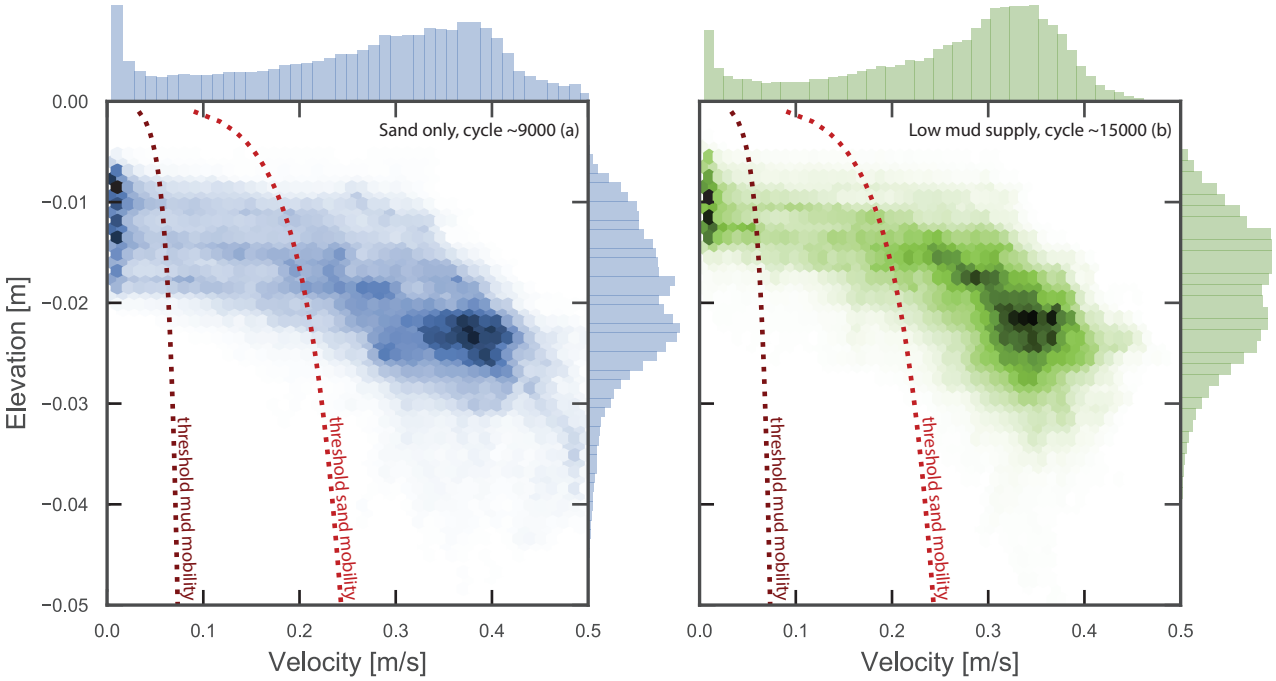

Figure 7: Scatter plot of elevation plotted against maximum surface velocity. Colour intensity and histograms on the sides indicate the velocity and elevation distribution. Still water level is at -0.005 m. Dotted lines indicate the critical threshold of motion for sand and mud. (a) Experiments with only sand at cycle 8863, (b) experiment with low mud supply at cycle 14975.

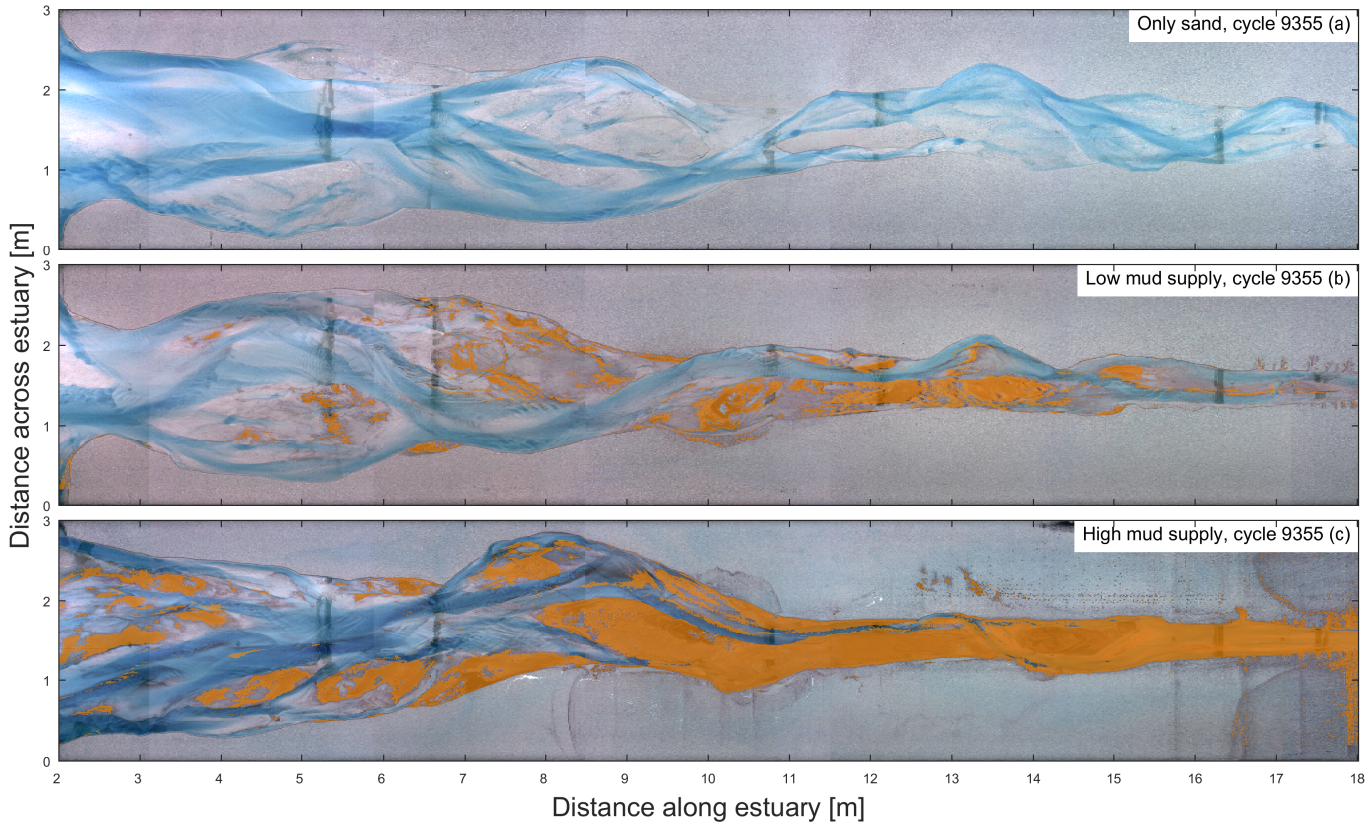

Figure 8: Spatial distribution of mud (classified in orange) in the estuary with: (a) only sand, (b) a low mud supply and (c) a high mud supply at cycle 9355.

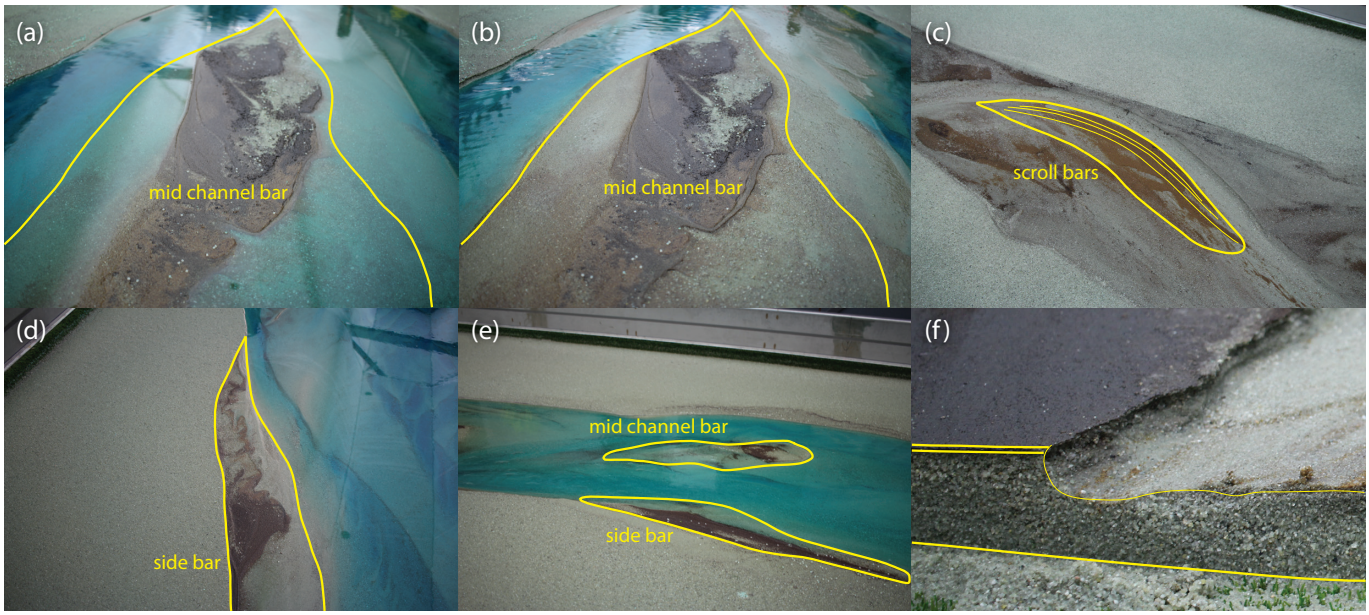

Figure 9: Detailed photographs of mud deposits in the experiments. a) Mudflat with high water, b) mudflat with low water, c) scrollbars, d) mudflat on the side, e) mudflat on a bar and on the side and f) cross-section of a channel with steep banks, indicating cohesive nature of the nutshell deposits.

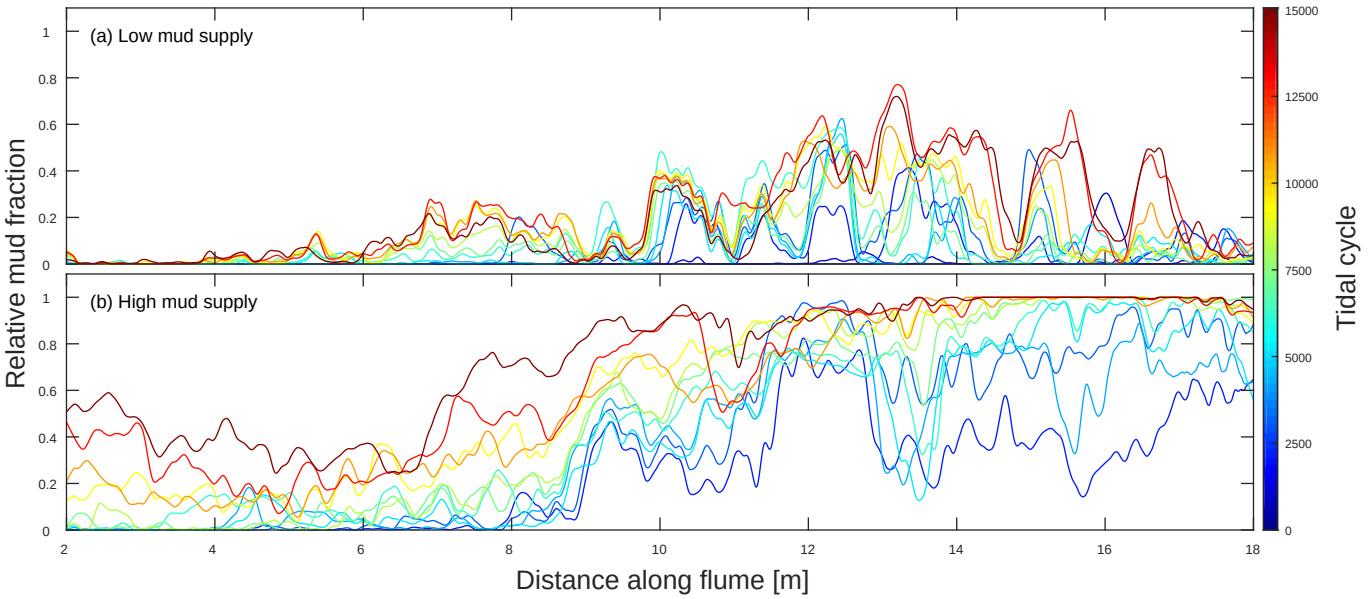

Figure 10: Mud cover relative to the estuary width along the estuary for (a) the experiment with a low mud supply and (b) the experiment with a high mud supply. Colours indicate different moments in time. The relative mud fraction was median filtered over a length of 200 pixels, which equals 0.2 m.

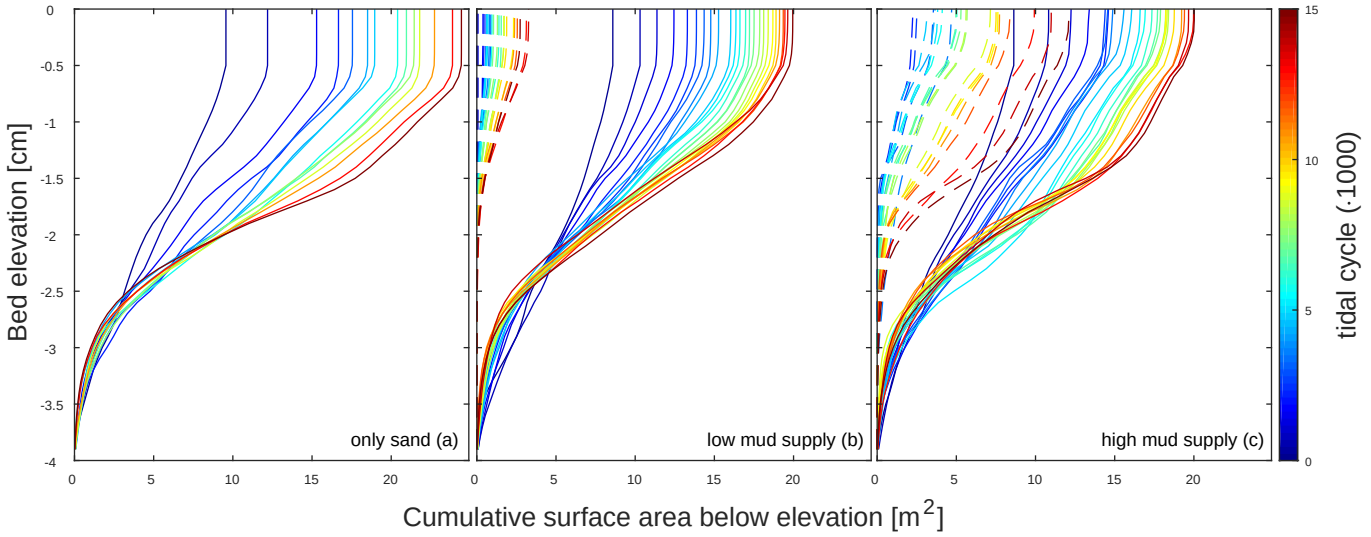

Figure 11: Cumulative total estuary area (solid) and mud covered area (dashed) below a certain elevation for the experiment with (a) only sand, (b) a low mud supply and (c) with a high mud supply. Colours indicate different moments in time.

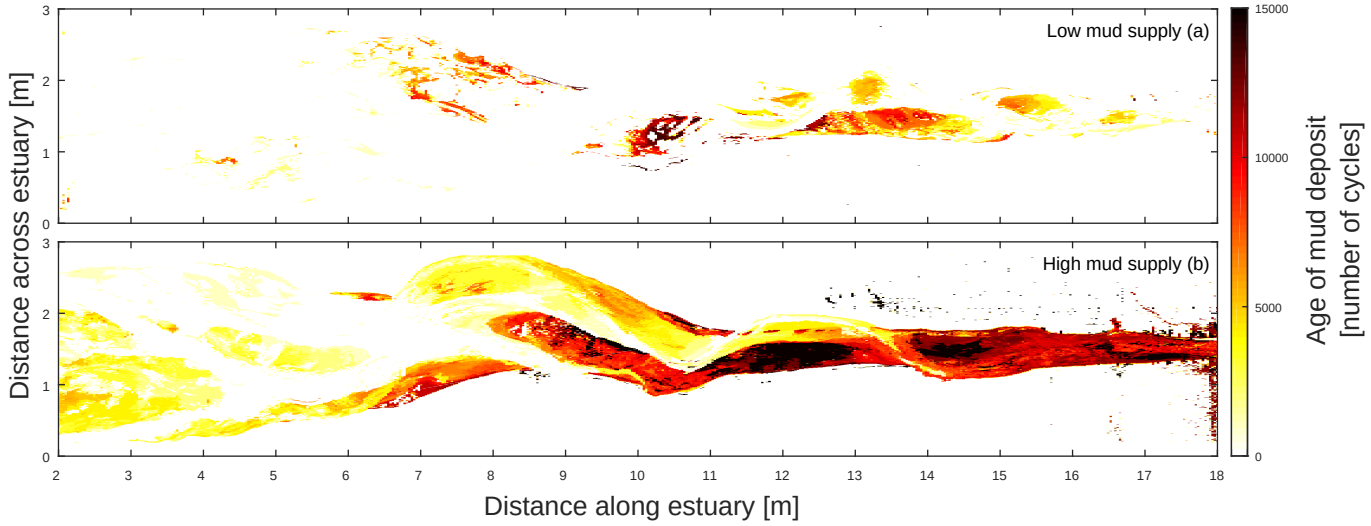

Figure 12: Spatial maps of the age of the mud deposits for the experiments with (a) a low mud supply and (b) a high mud supply. Darker colours indicate older deposits. (c,d) Histograms of maps (a,b) of mud age for the final situation.

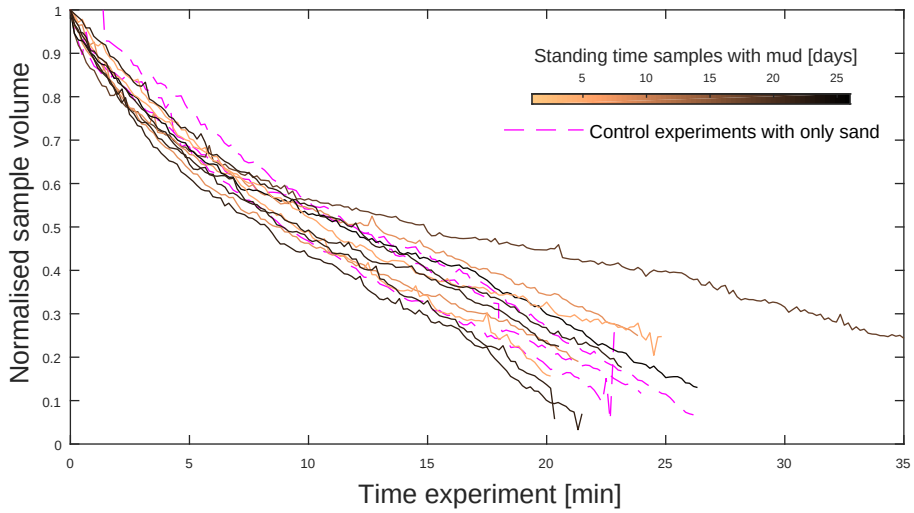

Figure 13: Volume of samples during bank erosion tests over time. Pink colours are control experiments with only sand. Orange-brown colours indicate the standing time of the samples with a mud layer before between making the sample and conducting the experiment. There are no differences in observed erosion rates for sediment type or standing time, which implies that bank erosion is not affected by mud.

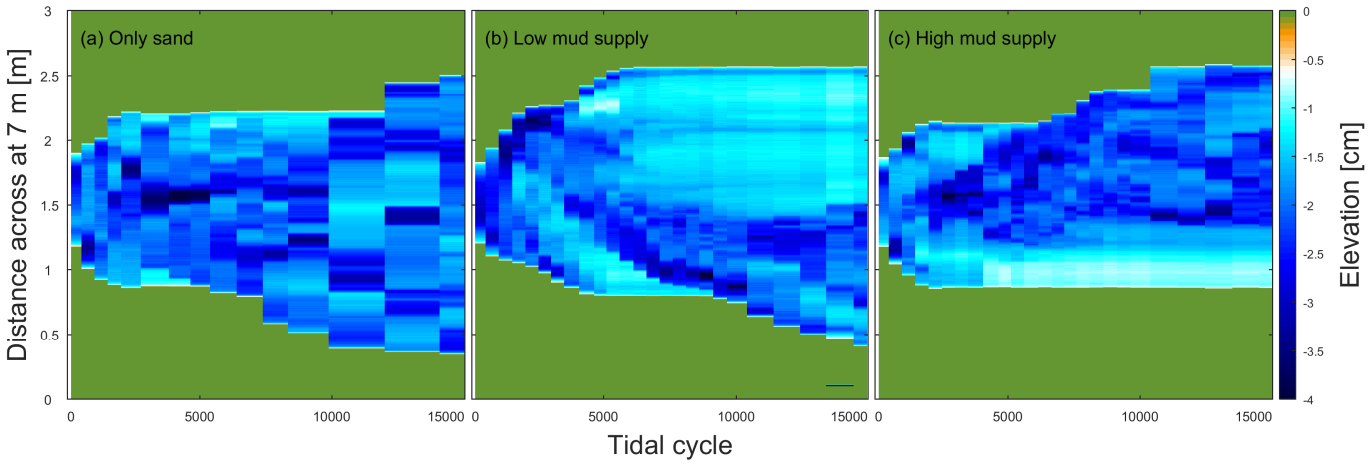

Figure 14: Timestacks: Bathymetric evolution of a cross section at 7 m over time for the experiment with (a) only sand, (b) a low mud supply, and (c) a high mud supply. Cross sections increase over time. Shallow areas in (b) and (c) are mudflats that prevent the channel migrating in that direction. The temporal resolution of the DEMs in (a) is too low to track the fast channel migration.

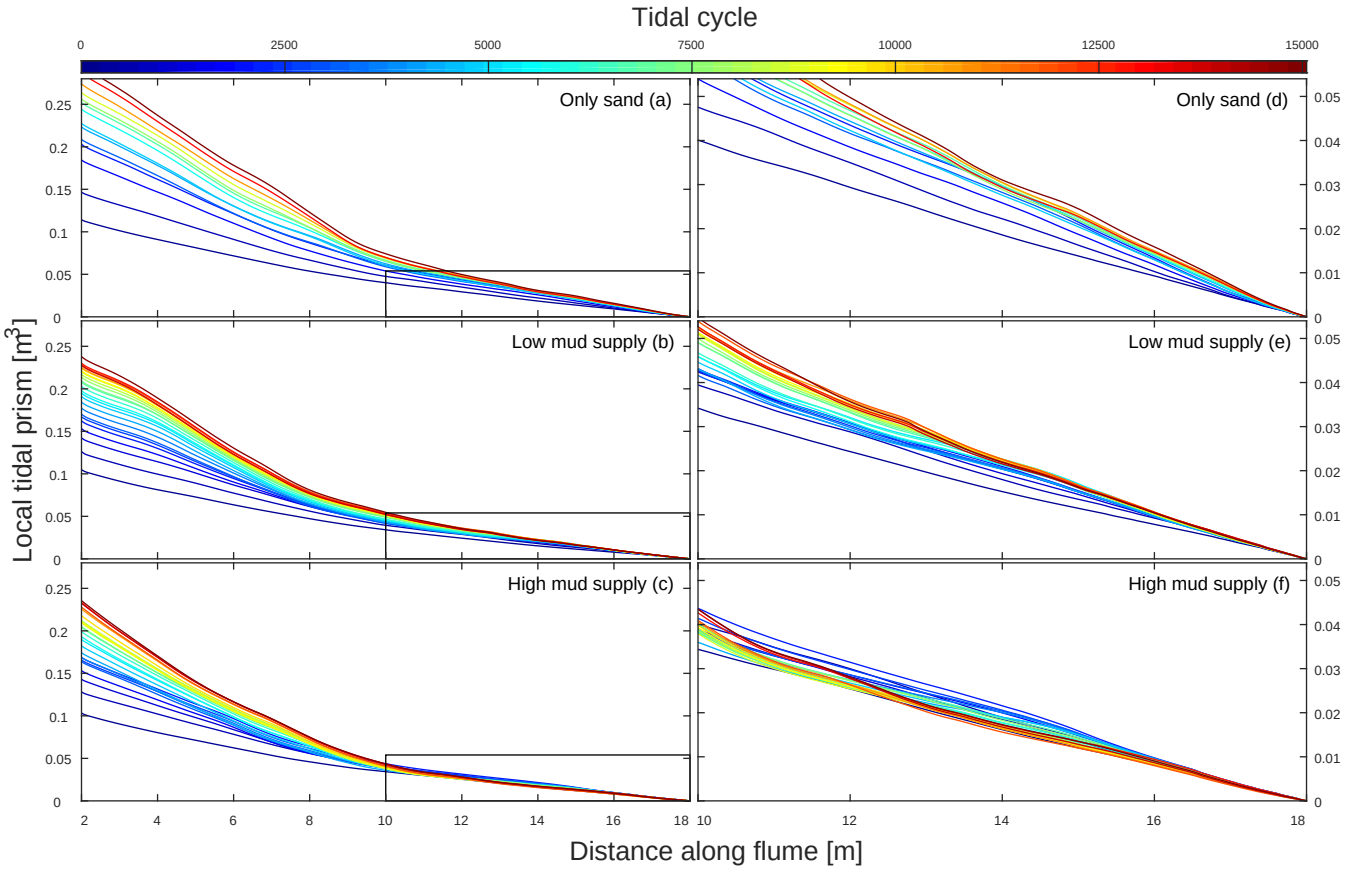

Figure 15: Locally defined tidal prism along the estuary at different moments in time for: (a) the experiment with only sand, (b) the experiment with a low mud supply, and (c) the experiment with a high mud supply. (d–f) Zoomed in on the upstream region of the estuaries. Tidal prism increases in the upstream region with high mud supply.

Supplementary material:
Effects of estuarine mudflat formation on tidal prism and large-scale morphology in experiments

Lisanne Braat *[1], Jasper R.F.W. Leuven[1], Ivar R. Lokhorst[1], and Maarten G. Kleinhans[1]

[1]Department of Physical Geography, Faculty of Geosciences, Utrecht University, Utrecht, The Netherlands

August 27, 2018

Table of contents

*L.Braat@uu.nl

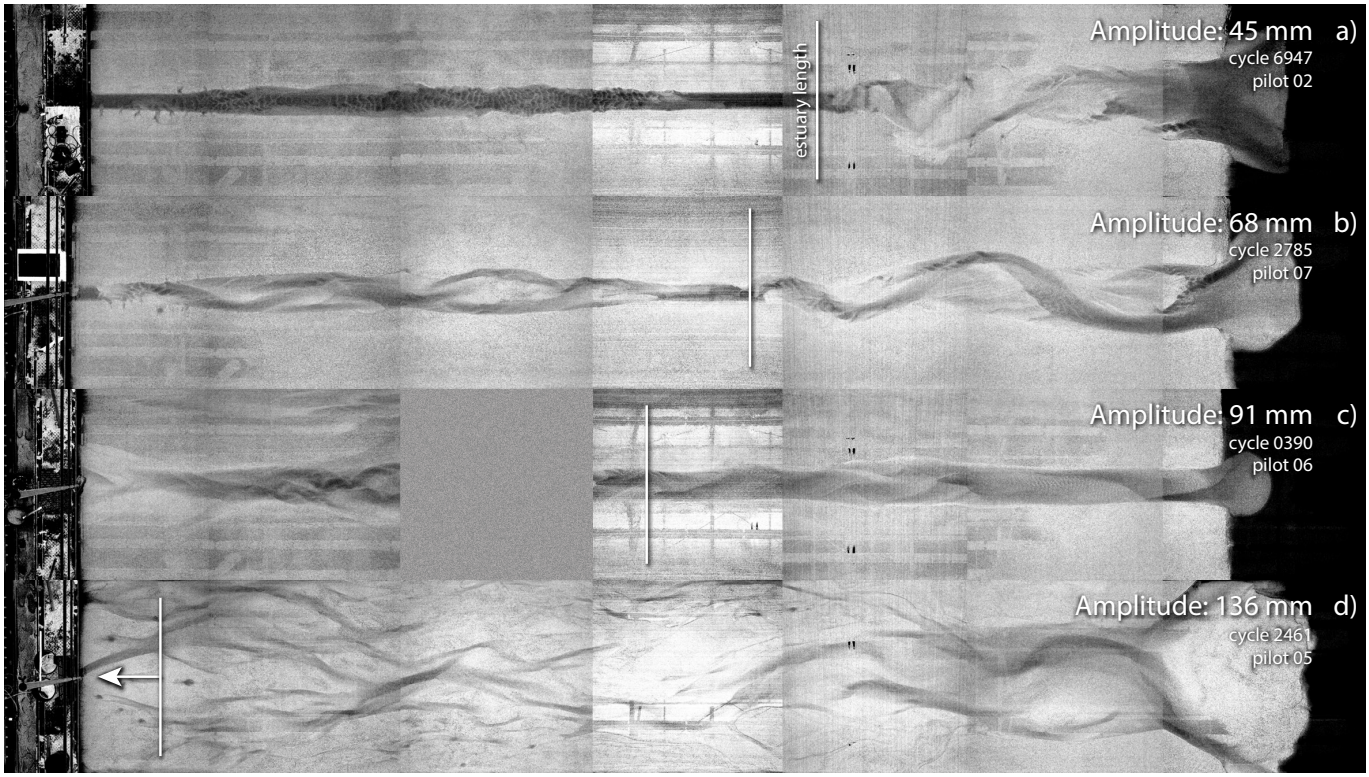

Figure S1: Top view of four pilot experiments (exp 2, 7, 6 and 5 in our lab numbering) illustrating the effect of tilting amplitude (45, 68, 91 and 136 mm) on estuary length indicated on the basis of visual observation of dynamics and morphology. The period of these experiments is 30 s rather than 40 s used in the main paper and the number of cycles for the four experiments are all different due to different run times. All experiments had the same river discharge of 250 Lh^{-1} and started with a straight channel of 195 m wide and 30 mm deep, no waves. Tilting amplitude, cycle number and experiment number are indicated at the seaward end of the estuary. Blue color band is shown here to indicate water depth. Note camera failure masked by grey box.

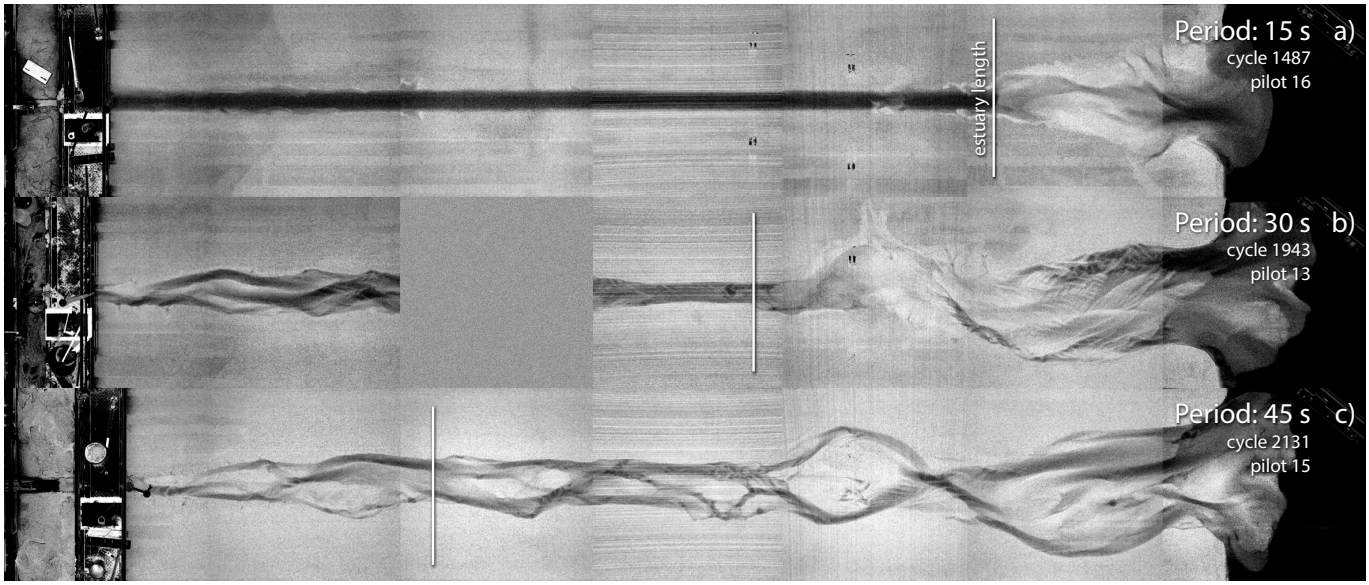

Figure S2: Top view of three pilot experiments (exp 16, 13 and 15 in our lab numbering) illustrating the effect of tilting period (15, 30 and 45 s) on estuary length indicated on the basis of visual observation of dynamics and morphology. Tilting amplitude is 68 mm, river discharge of 250 Lh^{-1} and the experiment started with a straight channel of 195 m wide and 30 mm deep, no waves. Tilting period, cycle number and experiment number are indicated at the at the seaward end of the estuary. Blue color band is shown here to indicate water depth. Note camera failure masked by grey box.

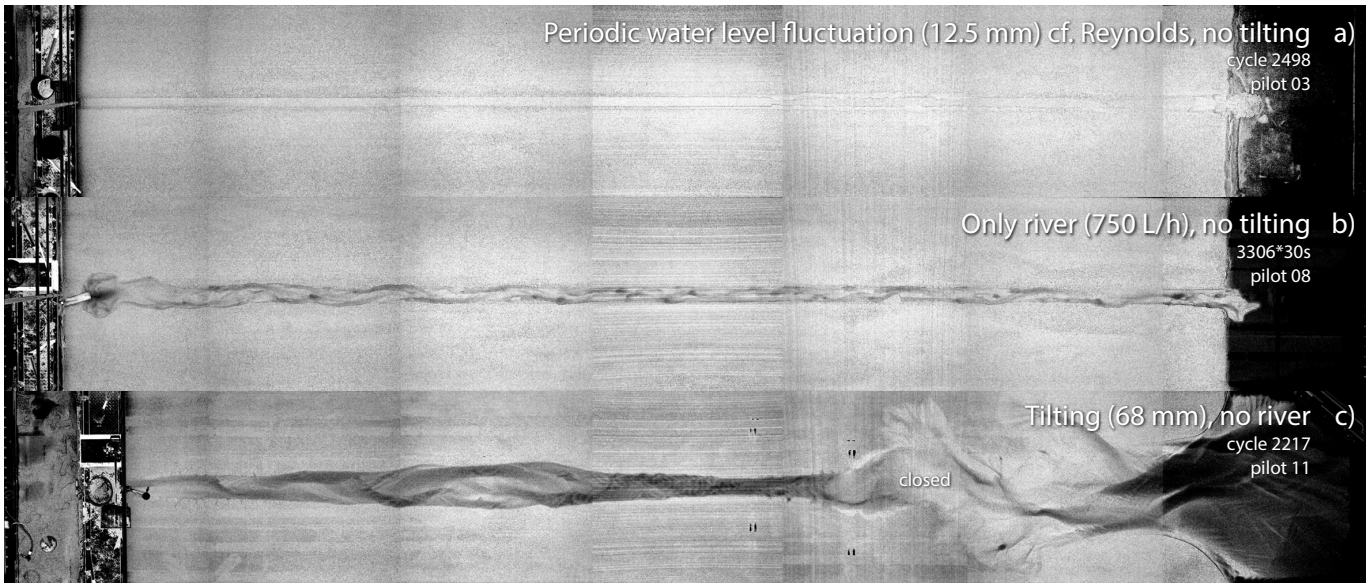

Figure S3: Top view of three pilot experiments (exp 3, 8 and 11 in our lab numbering) illustrating the effect of the principle of tilting the flume and the effect of river discharge. The periodic water level fluctuations (12.5 mm, 30 s) by the Reynolds method without tilting (a) and the river discharge (750 Lh^{-1}) without tilting (b) have almost no effect on the morphology on their own. In both cases a small delta of less than 0.25 m^2 developed initially and became static in the Reynolds experiment. Tilting the flume (68 mm, 30 s) without river discharge (c) however leads to a well-developed short tidal basin instead of an elongated estuary (compare to Figs S1,S2), showing that the minor river discharge in combination with the tides by tilting has a major effect on system length. All pilots started with a straight channel of 195 m wide and 30 mm deep, no waves. Cycle number and experiment number are indicated at the seaward end of the estuary. Blue color band is shown here to indicate water depth.